Pergamon

Geochimica et Cosmochimica Acta, Vol. 68, No. 21, pp. 4453–4468, 2004

0016-7037/04 $30.00 + .00

doi:10.1016/j.gca.2004.01.016

Pb isotopic heterogeneity in basaltic phenocrysts

JULIA G. BRYCE* and DONALD J. DEPAOLO

Center for Isotope Geochemistry, Department of Earth and Planetary Science, University of California, Berkeley CA 94720-4767, USA

(*Received July* 1, 2002; *accepted in revised form January* 20, 2004)

Abstract—The Pb isotopic compositions of phenocrystic phases in young basaltic lavas have been investigated using the Getty-DePaolo method (Getty S. J. and DePaolo D. J. [1995] Quaternary geochronology by the U-Th-Pb method. *Geochim. Cosmochim. Acta* **59,** 3267–3272), which allows for the resolution of small isotopic differences. Phenocryst, matrix, and whole rock analyses were made on samples from the 17 Myr-old Imnaha basalts of the Columbia River Group, a zero-age MORB from the Mid-Atlantic Ridge, and a ca. 260 kyr-old tholeiite from Mount Etna. Plagioclase feldspar phenocrysts have low-(U, Th)/Pb, and in each sample the plagioclase has significantly lower $^{206}Pb/^{207}Pb$ and $^{208}Pb/^{207}Pb$ values than whole rock, matrix, and magnetite-rich separates. The Pb isotopic contrast between plagioclase and matrix/whole rock is found in three samples with varying grain sizes (0.5–2 cm for the Imnaha basalt and MORB and <1 mm for the Etna sample) from different tectonic settings, suggesting that these results are not unique. The isotopic contrasts are only slightly smaller in magnitude than the variations exhibited by whole rock samples from the region. The Imnaha basalts also have Sr isotopic heterogeneity evident only in plagioclase phenocrysts, but the MORB and Etna lavas do not. The isotopic heterogeneities reflect magma mixing, and indicate that isotopically diverse magmas were mixed together just prior to eruption. The results reinforce indications from melt inclusion studies that magma source region isotopic heterogeneities have large amplitudes at short length scales, and that the isotopic variations imparted to the magmas are not entirely homogenized during segregation and transport processes. *Copyright © 2004 Elsevier Ltd*

1. INTRODUCTION

The chemical and isotopic compositions of basaltic lava erupted at Earth's surface result from fractionation and mixing processes that accompany melting of the mantle at depths of 50 to 150 km, transport toward the surface by porous flow and ascent through dikes, evolution in a magma chamber, and eruption. For basaltic magma in particular, it has generally been assumed that small-scale chemical and isotopic heterogeneities present in the mantle before melting are indiscernible in the lava erupted at the surface. Relatively inviscid basaltic magma should undergo homogenization in conduits and magma chambers that are traversed before eruption. Basaltic lavas are consequently regarded as homogeneous materials that can be adequately characterized by a single isotopic composition. Some chemical variability may be regenerated by partial crystallization before and during eruption, but this late-forming variability is superimposed on what is assumed to be a homogeneous magma composition.

The longstanding ideas about basalt magma homogeneity predate recent advances in the understanding of magma generation and transport (Richter and McKenzie, 1984; McKenzie, 1985; Ribe, 1985; Spiegelman, 1996). Nevertheless, there has been a persistent belief that magma erupted at Earth's surface should be highly homogenized in comparison to the volume of mantle from which the magma was extracted. Recent studies of melt inclusions in basaltic phenocrysts have revealed large chemical (e.g., Sours-Page et al., 1999; Sobolev et al., 2000) and isotopic variations among inclusions in both a suite of lavas, in the phenocrysts of one lava, and even within single olivine grains (Eiler et al., 1998; Saal et al., 1998). These results have, accordingly, challenged this concept of magma homogeneity and raised difficult questions about the nature of magma transport.

In magma types that are more "evolved," such as andesite and rhyolite, evidence of isotopic heterogeneity is fairly common (e.g., for review, Hawkesworth et al., 2000; Davidson et al., 2001). In more silicic magmas, heterogeneity resulting from magma mixing (e.g., Tepley et al., 1999), assimilation (e.g., Knesel et al., 1999), recharge (e.g., Davidson and Tepley, 1997), and radioactive decay (e.g., Christensen and DePaolo, 1993) is understandable. Magmas with these compositions often have an extended residence in magma chambers before eruption, the magma temperatures are relatively low, and accordingly magma viscosity is high and intracrystalline elemental diffusivities are low (cf. Hawkesworth et al., 2000). In contrast, few studies document isotopic differences among phenocrysts in less evolved magmas (e.g., Cortini and van Calsteren, 1985; Simonetti and Bell, 1994; Paslick et al., 1996). Where heterogeneity has been found, it typically involves xenocrysts or phenocrysts (up to several cm in diameter and/or zoned), suggestive of exceptionally long magma chamber residence times or open systems.

In this study, we examine Pb isotopic compositions of minerals in basaltic lavas. The objective of the study was to evaluate the possible application to basalts of a specialized U-Th-Pb chronometer for dating Quaternary rocks (Getty and DePaolo, 1995). A geologically meaningful date will result from this Getty-DePaolo technique only if there is a high degree of isotopic uniformity among mineral phases and quenched basaltic liquid (glass or groundmass) at the time of eruption. We have found that, at the level required for geochronologic applications and easily resolved with our analytical

* Author to whom correspondence should be addressed (julie.bryce@unh.edu).

techniques, minerals in basaltic lavas that we have investigated are grossly different in Pb isotopic composition. Plagioclase feldspar in particular is almost uniformly aberrant. Getty and DePaolo (1995) found a similar result in the phenocrystic plagioclase of a dacitic lava.

2. SAMPLE DESCRIPTIONS AND PREPARATIONS

The Imnaha basalt sequence was emplaced at ~17.5 Ma (Baksi, 1989; Hooper et al., 2002) and is the earliest of the Columbia River Basalt Group (CRBG) lavas. The two samples chosen for this study were collected by Dodson et al. (1997). Both are from the Rock Creek flows (as described in Hooper et al., 1984) and are plagioclase-phyric lavas, with plagioclase phenocrysts up to 2–3 cm and subordinate pyroxene and olivine. Sample CRB-14 is from a plagioclase-cumulate section of the Rock Creek 2 (RC2) flow of Hooper et al. (1984), whereas sample CRB-16 is from the Rock Creek 1 flow (RC1). Sample CRB-14 is fresh with very little evidence of weathering or deuteric alteration. CRB-16, however, does contain weathering products in the groundmass and as small veins in the plagioclase phenocrysts. The Imnaha basalts were erupted through lithosphere that was accreted during the Mesozoic (Kistler and Peterman, 1978), and unlike the CRBG lavas to the north erupted through the cratonic lithosphere, Imnaha basalts have isotopic compositions that indicate that they have been affected by minimal amounts of crustal contamination (Carlson et al., 1984; Chesley and Ruiz, 1998). Samples CRB-14 and CRB-16 have ε_{Nd} values of 3.7 and 3.1 respectively (Table 1), which are somewhat lower than the highest values measured in the Imnaha sequence, (which are >6.0), and hence could be argued to have been affected by some amount of crustal contamination. Sample CRB-14 was also found by Dodson et al. (1997) to have relatively high $^3He/^4He$ ($R/R_A = 11.5 \pm 0.8$) indicative of a plume source for the CRBG.

Sample NMNH 115087-2 is a plagioclase phyric MORB collected from a ridge crest dredging expedition at 22-23 °N along the Mid-Atlantic Ridge (Melson et al., 1968). The precise age of this sample is unknown, but as the lava was collected along the ridge axis, it is presumed to have an age of less than a few thousand years. The sample contains plagioclase phenocrysts (typically 0.5 to 1.0 cm), which are slightly zoned and thinly rimmed. The largest plagioclase phenocrysts contain small melt inclusions as well as inclusions of olivine and earlier-crystallizing plagioclase feldspar up to ~400 μm in size. Skeletal plagioclase crystals up to a few hundred microns in size dominate the groundmass. This sample appears very fresh in thin section, but the whole rock sample was nevertheless leached to evaluate seawater-derived components.

Sample SdV-1 is a subalkaline lava erupted at ~260 ka (Gillot et al., 1994) from fissures to the south and southwest of the present-day Mt. Etna near the town of Stazione di Valcorrente (Romano, 1982; Bryce, 1998). This lava is a pigeonite tholeiite with ca. 10% small (<2 mm) olivine and clinopyroxene microphenocrysts, subordinate plagioclase (<1 mm) crystals, and a groundmass consisting of ~50 to ~200 μm laths of plagioclase intergrown with olivine and pyroxene. Because of the small size of the crystals in this rock, pure mineral separates were difficult to obtain.

3. ANALYTICAL PROCEDURES

3.1. Sample Preparation and Analysis

Specimens for this study were crushed by hand to ~3 mm chips, ultrasonically leached in 3 N HNO_3 to remove surficial contaminants and then further processed in agate and alumina mortars and pestles. Grains were then separated into phases desired for study by magnetic separations and, when feasible, iterative hand picking. Mineral separates were then digested in a HF-HNO_3-$HClO_4$ mixture. Splits of the dissolved solutions were subsequently spiked with ^{205}Pb, ^{229}Th, and ^{233}U for concentration determination. The sample was then loaded in dilute HBr onto Bio-Rad AG1×8 anion exchange resin for chemical separation of Pb. The U and Th were subsequently separated using Eichrom TRU Spec Resin using slight modifications of the technique described by Luo et al. (1997). Typical procedural blanks were <200 pg for Pb, <10 pg for U, and <5 pg for Th. The U and Th blanks are negligible for the purposes of this study. The Pb blanks, although larger, are also too small to affect the results, since the total amount of Pb in the samples processed was always greater than 200 ng, or $>10^3$ times larger than the blank contribution.

Lead concentrations were determined by isotope dilution using a VG Sector 54 multicollector mass spectrometer operating in static mode. An initial $^{207}Pb/^{204}Pb$ normalizing value was obtained from the spiked analysis of the low U-Th/Pb phase; this discrimination factor was later refined by subsequent analyses of an unspiked aliquot of the low U-Th/Pb phase. High precision, normalized Pb isotopic ratios are measured on ~200 ng Pb loads using a multicollector mass spectrometer in dynamic mode. Mass discrimination corrections are done using the "exponential" correction law (Russell et al., 1978). Relatively large ion beams ($^{204}Pb+ \geq 0.1 \times 10^{-11}$ amp) were required to minimize drifts (0.01%) in the corrected ratios during the run due to an unidentified interference, presumably a hydrocarbon compound (cf. Getty and DePaolo, 1995; Todt et al., 1996). The average NIST SRM 981 ratios determined from the standards analyses conducted in static mode were (with corresponding 2σ, n = 12): $^{206}Pb/^{204}Pb$ = 16.903 ± 0.033; $^{207}Pb/^{204}Pb$ 15.446 ± 0.043; $^{208}Pb/^{204}Pb$ 36.565 ± 0.129. Using the NIST SRM-981 values from Thirlwall (2000), these values correspond to an average fractionation correction of 0.17 ± 0.06%/amu. These static measurements were mainly used to calculate the concentrations of Pb by isotope dilution and to establish a baseline $^{207}Pb/^{204}Pb$ normalizing value, as discussed above.

High precision $^{207}Pb/^{204}Pb$-normalized Pb isotopic ratios for NIST SRM-981 were evaluated with the multicollector in dynamic mode, using a correction for mass discrimination based on a static measurement of $^{207}Pb/^{204}Pb$ and the accepted value of $^{207}Pb/^{204}Pb = 15.4956$ (cf. Thirlwall, 2000). Average values were $^{206}Pb/^{207}Pb = 1.0934 \pm 0.0002$ (2σ, n = 16) and $^{208}Pb/^{207}Pb = 2.3699 \pm 0.0004$ (2σ, n = 16). The reproducibility for standards analyzed within the same 24-h period was better by at least a factor of two. As is evident in the following discussions, we can capably resolve the differences in $^{206}Pb/^{207}Pb$ and $^{208}Pb/^{207}Pb$ at a much better precision than is required to observe the variations in our samples.

Uranium and thorium analyses were performed on a VG

Table 1. U-Th-Pb, Rb-Sr, and Nd isotopic data for basalts.

Sample description	$^{238}U/^{207}Pb$	2 SE (M)	$^{232}Th/^{207}Pb$	2 SE (M)	$^{206}Pb/^{207}Pb$[a]	2 SE (M)[b]	$^{208}Pb/^{207}Pb$[a]	2 SE (M)	$^{206}Pb/^{207}Pb_i$[c]	$^{208}Pb/^{207}Pb_i$[c]	$[^{207}Pb]$ $\mu g/g$	$^{87}Sr/^{86}Sr$[d]	2 SE (M)	$^{87}Rb/^{86}Sr$	2 SE (M)	[Sr] $\mu g/g$	σ_{Nd}[e]
CRB-14																	
WR[f]	1.020	0.005	3.405	0.015	1.22054	0.00002	2.4725	0.0001	1.2180	2.4697	0.93	0.704186	0.000007	0.0988	0.0005	295	3.7[g]
WR (split of same solution)	—	—	—	—	1.22063	0.00003	2.4724	0.0001	—	—	—	—	—	—	—	—	—
Mt-rich	0.805	0.002	2.629	0.014	1.22748	0.00009	2.4689	0.0002	1.2255	2.4667	0.83	0.704151	0.000011	0.1635	0.0011	226	—
plag	0.105	0.000	0.205	0.000	1.21952	0.00003	2.4680	0.0001	1.2193	2.4679	0.15	0.703992	0.000010	0.0042	<0.0001	689	4.1
CRB-16																	
WR	0.979	0.002	3.557	0.034	1.22212	0.00005	2.4733	0.0001	1.2197	2.4704	1.06	0.704371	0.000011	0.1474	0.0008	436	—
WR (solution 2)	0.934	0.007	3.565	0.033	1.22205	0.00009	2.4728	0.0004	1.2197	2.4699	1.02	—	—	—	—	—	—
WR (solution 2 split)	—	—	—	—	1.22179	0.00008	2.4717	0.0003	—	—	1.02	—	—	—	—	—	—
Mt-rich fraction soln 1	0.908	0.004	3.453	0.024	1.22302	0.00004	2.4731	0.0002	1.2208	2.4703	1.00	—	—	—	—	—	—
Mt-rich fraction soln 2	0.935	0.004	3.449	0.019	1.22304	0.00002	2.4727	0.0001	1.2207	2.4699	1.05	0.704354	0.000011	0.2036	0.0007	118	—
Mt-rich fraction soln 3	1.095	0.001	3.551	0.002	1.22073	0.00004	2.4711	0.0001	1.2180	2.4682	0.49	0.704432	0.000011	0.2010	0.0006	306	—
plag	0.130	0.001	0.274	0.000	1.21446	0.00001	2.4635	0.0000	1.2141	2.4632	0.18	0.703981	0.000008	0.0067	0.0001	1027	0.6
Wr[h]	—	—	—	—	—	—	—	—	—	—	—	0.704392	0.000010	0.1395	—	259	3.1
Mt-rich[h]	—	—	—	—	—	—	—	—	—	—	—	0.704384	0.000010	0.1550	—	217	3.2
NM5087-Mid Atlantic Ridge Basalt																	
WR	0.661	0.003	1.357	0.001	1.19186	0.00003	2.4428	0.0001	—	—	0.283	0.702555	0.000010	0.0206	<0.0001	124	—
WR[i]	—	—	—	—	1.19275	0.00003	2.4440	0.0001	—	—		0.702497	0.000010	—	—	—	—
Mt-rich[i]	0.493	0.002	1.159	0.016	1.20147	0.00002	2.4456	0.0001	—	—	0.399	0.702572	0.000010	0.0298	0.0001	155	—
plag[i]	0.091	0.000	0.125	0.000	1.18453	0.00004	2.4373	0.0002	—	—	0.045	0.702380	0.000010	0.0017	<0.0001	203	—
Wr[h]												0.702397	0.000008	0.0139	—	—	10.0
SdV1-Mt. Etna																	
magnetic split, 150–300 μm	1.601	0.008	6.793	0.034	1.24229	0.00019	2.4993	0.0004	1.2422	2.4992	0.203	0.703178	0.000005	—	—	—	—
magnetic split, 75–150 μm	1.895	0.009	8.223	0.041	1.24678	0.00003	2.5030	0.0001	1.2467	2.5028	0.174	0.703201	0.000005	—	—	—	—
weakly magnetic, 150–300 μm	1.361	0.007	5.948	0.030	1.23987	0.00015	2.4962	0.0006	1.2398	2.4962	0.171	—	—	—	—	—	—
weakly magnetic, 75–150 μm	1.473	0.007	6.314	0.032	1.24361	0.00008	2.5004	0.0003	1.2435	2.5003	0.164	0.703184	0.000004	—	—	—	—
Plag-rich, 75 to 300 μm (separate crushed sample)	0.221	0.001	0.996	0.005	1.20190	0.00009	2.4653	0.0003	1.2019	2.4653	0.821	0.703208	0.000006	—	—	—	—
nonmagnetic split, 75 to 300 μm[j]	—	—	—	—	1.2118	0.00010	2.4784	0.0007	—	—	—	—	—	—	—	—	—
crushed WR. 75 to 300 μm[j]	—	—	—	—	1.2514	0.00017	2.5062	0.0010	—	—	—	—	—	—	—	—	—

[a] $^{206}Pb/^{207}Pb$ are reported normalized to $^{207}Pb/^{204}Pb = 15.49784$ for the CRB and NMNH samples and $^{207}Pb/^{204}Pb = 15.60932$ for the SdV1 sample.

[b] Reproducibility (2σ) over a two-year period on $^{207}Pb/^{204}Pb$ normalized NIST-SRM 981 is ± 0.0002 for $^{206}Pb/^{207}Pb$ and ± 0.0004 for $^{208}Pb/^{207}Pb$. Within session reproducibility for NIST-SRM 981 typically <0.0001 for $^{207}Pb/^{204}Pb$ and ~ 0.0002 for $^{208}Pb/^{204}Pb$.

[c] Initial $^{206}Pb/^{207}Pb$ given for the CRB and SdV samples using t = 17 Mn and t = 260 ka. See text for discussion.

[d] Reported relative to Standard values for NIST-SRM 987 of 0.710250.

[e] Reported relative to BCR $\sigma_{Nd} = 0$.

[f] WR = whole rock; Mt = Magnetite; Plag = plagioclase.

[g] Reported by Dodson et al. (1997): this value is reported relative to BCR $\sigma_{Nd} = 0$.

[h] Leached in 6 N HCl-7 N HNO_3.

[i] Leached in 0.1 N HNO_3.

[j] Splits made from a second crushate of the large hand sample. The chips were subject to the same leaching treatment as the ones above, but were then subsequently leached in warm 5 N HCl for ~ 1 hour.

Note: These Pb isotopic data are normalized and should therefore be treated as model numbers. See the text and Getty and DePaolo (1995,2000) for further discussion.

single collector mass spectrometer equipped with a Daly detector. For Uranium analyses, the filament temperature was ~1600°C whereas Th ran at higher temperatures. Fractionation corrections used for the concentration determinations were 0.10 ± 0.05%/amu for U and Th.

Samples for Sr isotopic study were prepared using standard ion chromatographic separation techniques (Bio-Rad AG50 and Eichrom Sr spec resins). Strontium isotopic measurements were made on the VG sector 54 multicollector mass spectrometer in dynamic mode. Isotopic fractionation was corrected using $^{86}Sr/^{88}Sr = 0.1194$, and the $^{87}Sr/^{86}Sr$ values reported in Table 1 are normalized to NIST SRM-987 values of 0.710250 from a long-term average of 0.710280.

Preparation of samples for Nd isotopic study was carried out using standard ion chromatographic procedures described in DePaolo (1978). Purified Nd salts were then loaded in 5 N HNO_3 onto rhenium filaments; Nd was run as NdO^+ in an environment $\sim 10^{-6}$ mbar oxygen pressure. Nd isotopic measurements were also made on the multicollector mass spectrometer operating in dynamic mode. Nd isotopic compositions were normalized to $^{146}Nd/^{142}Nd = 0.636151$ to correct for within-run fractionation and are reported in Table 1 relative to the chondritic uniform reservoir (CHUR) value for $^{143}Nd/^{144}Nd$ of 0.511836. Two different Nd isotopic standards were analyzed in the same time period as that of the samples reported in Table 1. The mean values determined for these standards were $^{143}Nd/^{144}Nd = 0.510979 \pm 0.000002$ (2 σ, n = 4) for the Berkeley Nd standard and $^{143}Nd/^{144}Nd = 0.511878 \pm 0.000002$ (2 σ, n = 2) for BCR-1. The average Nd isotopic composition of BCR-1 measured contemporaneously with the analysis of the CRB-14 WR sample reported by Dodson et al. (1997) was $^{143}Nd/^{144}Nd = 0.511871$ (2 $\sigma = 0.000003$, n = 6). All ε_{Nd} values reported in Table 1 are normalized to the value of $^{143}Nd/^{144}Nd = 0.511836$ ($\varepsilon_{Nd} = 0$) for BCR-1.

Mineral compositions were determined with a Cameca SX-51 at the University of California Department of Earth and Planetary Science Electron Microprobe Facility. Standards of similar composition were used to minimize matrix corrections. Silicate analyses were conducted using a 5 μm beam at 15 kV and 20 nA. Major element compositions of sulfide inclusions were conducted using a focused beam at 12 kV and 15 nA, whereas the analyses of minor elements in the sulfides were made using a 20 kV and 30 nA beam set-up. Because the grains were so small, we were able only to identify the sulfide phases and obtain order-of-magnitude information about the Pb content. Count times for elemental analyses ranged from 10–50 s.

3.2. U-Th-Pb System in Terms of $^{206}Pb/^{207}Pb$ and $^{208}Pb/^{207}Pb$ Ratios

The Getty-DePaolo Quaternary technique uses the ratio $^{207}Pb/^{204}Pb$ to correct for mass discrimination and monitors changes in the ratio $^{206}Pb/^{207}Pb$ relative to the $^{238}U/^{207}Pb$ ratio. The $^{206}Pb/^{207}Pb$ ratio is used because most (>95%) of the radiogenic Pb from recent U decay is ^{206}Pb. The exact equation for the evolution of the $^{206}Pb/^{207}Pb$ ratio in a mineral with time is (Getty and DePaolo, 1995, 2000):

$$\frac{^{206}Pb}{^{207}Pb}(t) = \frac{^{206}Pb}{^{207}Pb}(0) + \frac{^{238}U}{^{207}Pb}(t) \times \left[(e^{\lambda_{238}t} - 1) - \frac{^{206}Pb}{^{207}Pb}(0) \frac{^{235}U}{^{238}U} (e^{\lambda_{235}t} - 1) \right] \quad (1)$$

where t = 0 is the time of formation of the mineral. This system behaves like any other isochron method (cf. Dickin, 1995). The effective decay constant is different from the actual decay constant of ^{238}U due to the small contribution of ^{235}U decay to ^{207}Pb. The effective decay constant for ^{238}U decay is:

$$\lambda^*_{238} = \lambda_{238} - \lambda_{235}\left(\frac{^{206}Pb/^{207}Pb(0)}{137.88}\right) \quad (2)$$

where 137.88 is the modern ratio $^{238}U/^{235}U$. By correcting the mass spectrometer data using the normalizing ratio $^{207}Pb/^{204}Pb_{norm}$, differences in $^{206}Pb/^{207}Pb$ between phases can be determined to about ±0.00002 under favorable conditions, which corresponds to an age resolution of $\Delta t \approx 50$ kyr for $\Delta^{238}U/^{207}Pb \approx 1.6$ (i.e., $\Delta\mu \approx 25$). Use of an imprecise value of $^{207}Pb/^{204}Pb_{norm}$ does not significantly affect the measured differences in $^{206}Pb/^{207}Pb$ between phases in the same rock. Likewise, irregularities in the decay series are relatively unimportant (cf. Getty and DePaolo, 1995).

An equation analogous to Eqn. 2 above can be written to describe the evolution of $^{208}Pb/^{207}Pb$ with time:

$$\frac{^{208}Pb}{^{207}Pb}(t) = \frac{^{208}Pb}{^{207}Pb}(0) + \frac{^{232}Th}{^{207}Pb}(t) \times \left[(e^{\lambda_{232}t} - 1) - \frac{^{208}Pb}{^{207}Pb}(0) \frac{^{235}U}{^{232}Th} (e^{\lambda_{235}t} - 1) \right]. \quad (3)$$

For minerals having Th/U ≥ 6.7, the percentage increase of the $^{208}Pb/^{207}Pb$ ratio per unit time is larger than that for the $^{206}Pb/^{207}Pb$. The Th-Pb method may also prove advantageous because of the relative geochemical immobility of Th and because the ^{232}Th-^{208}Pb decay chain lacks long-lived intermediate daughter products. Measurements of $^{208}Pb/^{207}Pb(t)$ and $^{232}Th/^{207}Pb(t)$ for multiple mineral phases will not necessarily fall upon a single line when plotted against one another because of the dependence of the bracketed term in Eqn. 3 on U/Th.

The use of $^{206}Pb/^{207}Pb$ and $^{208}Pb/^{207}Pb$ values is not the standard procedure for Pb isotope studies. We use Figure 1 to show how these ratios vary on a more typical plot of $^{206}Pb/^{204}Pb$ versus $^{207}Pb/^{204}Pb$. Lower $^{206}Pb/^{207}Pb$ ratios correspond to older Pb model ages, but they can be produced in magmas by adding material with low $^{206}Pb/^{204}Pb$, adding material with high $^{207}Pb/^{204}Pb$, or combinations that include the addition of material with both high $^{206}Pb/^{204}Pb$ and high $^{207}Pb/^{204}Pb$. Although from the discussion above it is clear that this technique was developed for geochronology, it also can provide information about petrogenetic history. If phases do not define an isochron with geochronologic meaning, this technique can be used as a petrogenetic tracer to investigate the initial state of $^{206}Pb/^{207}Pb$ or $^{208}Pb/^{207}Pb$ disequilibrium. Normalizing with $^{207}Pb/^{204}Pb$ values may provide a means for correcting for fractionation in mineral-whole rock systems using MC-ICP-MS analytical techniques.

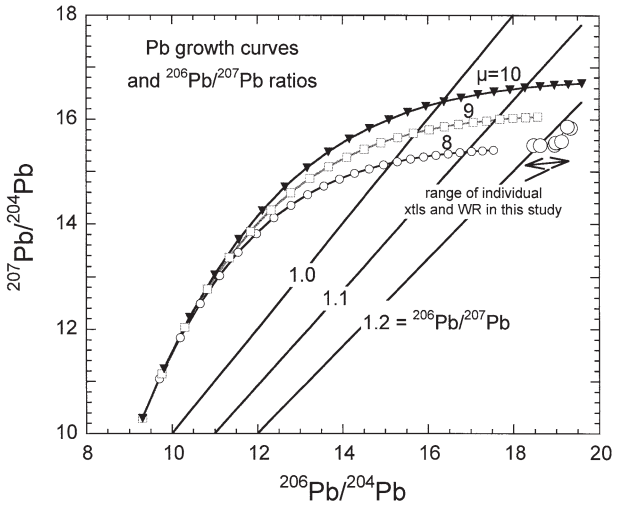

Fig. 1. Correspondence between $^{206}Pb/^{207}Pb$ ratios and the standard terrestrial growth curves for uranogenic Pb isotopes for different values of μ, which is the modern value of $^{238}U/^{204}Pb$. The unfilled circles show the values measured for the materials discussed in this work.

4. RESULTS

4.1. Pb and Sr Isotopic Data

For the Imnaha lavas we measured whole rocks, plagioclase separates, and magnetic separates. The data are given in Table 1 and shown in Figures 2 and 3 on standard isotopic evolution diagrams used for geochronology. For sample CRB-14, the plagioclase separate has significantly lower $^{206}Pb/^{207}Pb$, and slightly higher initial $^{208}Pb/^{207}Pb$ (i.e., corrected to 17 Ma) than the whole rock (WR). The plagioclase Pb concentration is ~6 times lower than the WR concentration, so the plagioclase phenocrysts contain only a few percent of the Pb in the rock. The magnetite separates are also distinct from the WR values, shifted in the same direction isotopically as the plagioclase, but by different amounts. The plagioclase and magnetite-rich fraction separates for CRB-14 also have lower initial $^{87}Sr/^{86}Sr$ than the WR sample (Fig. 2c). For sample CRB-16, the plagioclase separate has both lower $^{206}Pb/^{207}Pb$, and lower initial $^{208}Pb/^{207}Pb$ than the whole rock. The magnetite-rich fractions and the crushed whole rock show some variability, but there is no consistent difference between them. The plagioclase of CRB-16 has a lower $^{87}Sr/^{86}Sr$ than the whole rock, whereas the magnetite-rich separate and whole rock have indistinguishable $^{87}Sr/^{86}Sr$. Leaching of whole rock and magnetite-rich separates of CRB-16 resulted in no significant change in the measured $^{87}Sr/^{86}Sr$ (Table 1) relative to unleached samples.

The MORB sample also displays initial Pb isotopic heterogeneity (Table 1; Fig. 4). For both $^{206}Pb/^{207}Pb$ and $^{208}Pb/^{207}Pb$, the plagioclase has a lower value and the magnetite has a higher value than the whole rock (Figs. 4a,b). In this sample, as with the CRB samples, the Pb concentration in plagioclase is ~6 times lower than the whole rock values and hence the plagioclase phenocrysts account for only ~2% of the total Pb budget of the rock. A sample of groundmass chips leached with 0.1 N HNO_3 resulted in little change (a small increase) to the Pb isotopic ratios, but a significant decrease in the $^{87}Sr/^{86}Sr$. Further leaching of the whole rock with 6 N HCl–7 N HNO_3 mixture lowered the $^{87}Sr/^{86}Sr$ so that it was identical to that of the plagioclase (Fig. 4c). Hence it appears that the whole rock (WR) Sr isotopic value is elevated only as a result of exchange with seawater, and there is no evidence for phenocryst-matrix Sr isotopic disequilibrium.

The Pb isotopic data for the Etna tholeiite are especially remarkable (Fig. 5). In this sample, magnetic groundmass sam-

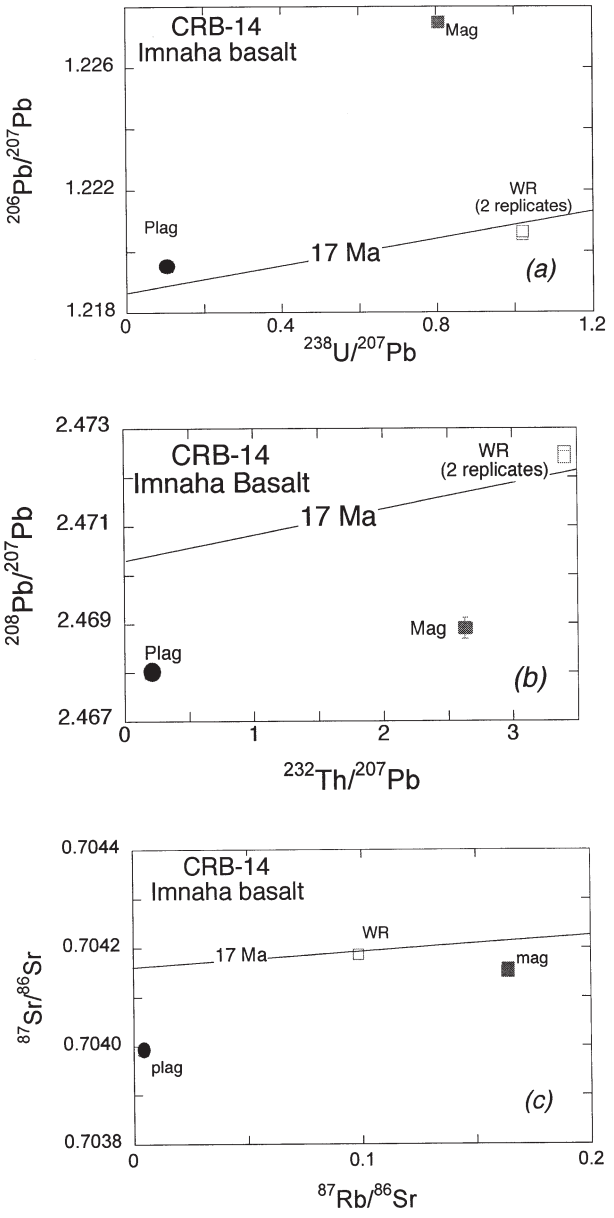

Fig. 2. Pb and Sr isotopic data of mineral fractions and whole rock from sample CRB-14, a sample from the Imnaha basalt of the Columbia River Basalt Group lavas. (a) $^{206}Pb/^{207}Pb$ vs. $^{238}U/^{207}Pb$ isochron; (b) $^{208}Pb/^{207}Pb$ vs. $^{232}Th/^{207}Pb$ isochron; (c) $^{87}Sr/^{86}Sr$ vs. $^{87}Rb/^{86}Sr$ isochron diagram. Superimposed on the data are lines depicting isochrons corresponding to an age of 17 Ma. Open squares symbolize plagioclase separates; filled squares symbolize WR crushate; and filled circles represent the magnetic fraction from the basaltic lavas. In this figure and those that follow, error bars are depicted when they are larger than the size of the data marker.

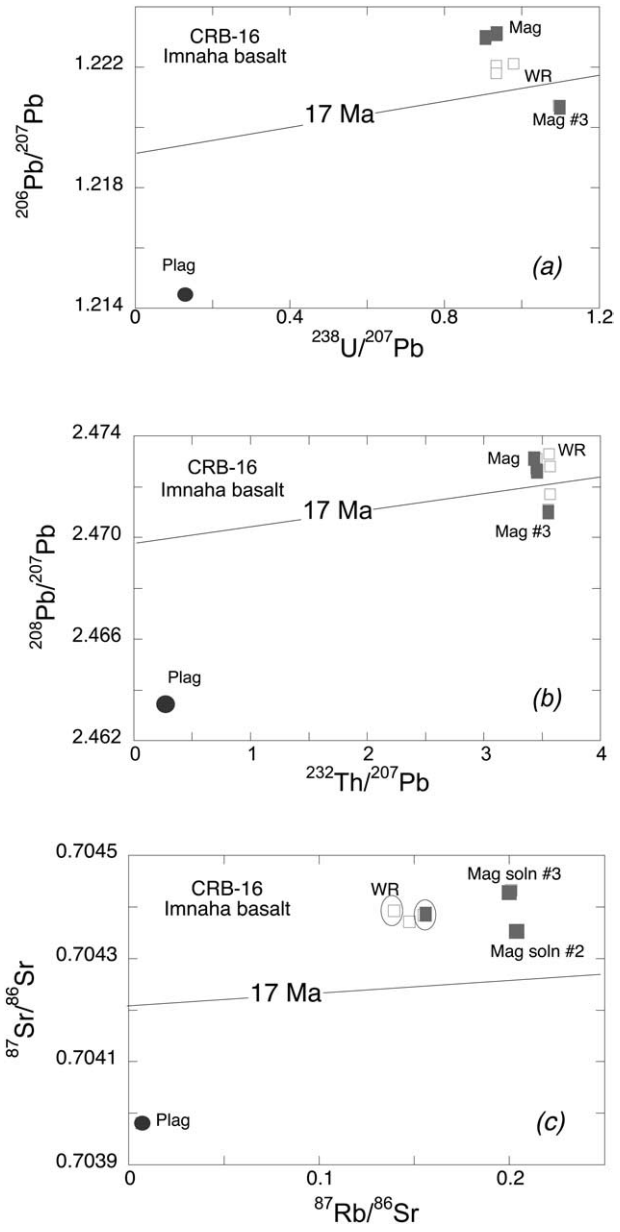

Fig. 3. Pb and Sr isotopic data of mineral fractions and whole rock from sample CRB-16 of the Imnaha basalt of the Columbia River Basalt Group. (a) $^{206}Pb/^{207}Pb$ vs. $^{238}U/^{207}Pb$ isochron; (b) $^{208}Pb/^{207}Pb$ vs. $^{232}Th/^{207}Pb$ isochron; (c) $^{87}Sr/^{86}Sr$ vs. $^{87}Rb/^{86}Sr$ isochron diagram. As with Figure 2, superimposed on the data are lines depicting isochrons corresponding to an age of 17 Ma.

ples show significant variations of both $^{206}Pb/^{207}Pb$ and $^{208}Pb/^{207}Pb$, but those differences are dwarfed by the large difference between the nonmagnetic (feldspar-rich) fraction and the magnetic groundmass separates. In contrast to the other samples, the feldspar crystals in the SdV lava are small (~1 mm size maximum). The Sr isotopic differences between the magnetic separates overlap at the level of reproducibility (0.000018) we have established in recent studies (e.g., DePaolo et al., 2001).

The isotopic differences between feldspar phenocrysts and whole rocks (or groundmass) are summarized in Figure 6. The $^{208}Pb/^{207}Pb$ and $^{206}Pb/^{207}Pb$ differences are well correlated (Fig. 6a). Phenocryst size and isotopic contrast are anticorrelated. There is also no correlation between the magnitude of the Pb isotopic and Sr isotopic contrasts (Fig. 6b).

In Figures 7 to 9, we compare the range of Pb and Sr isotopic values measured in our samples with the range of values measured in rocks of the volcanic sequences in which our samples occur. In making these comparisons, we have renormalized the literature Pb data to the same values of $^{207}Pb/^{204}Pb$ that we used (Table 1). For the Imnaha basalts, the differences

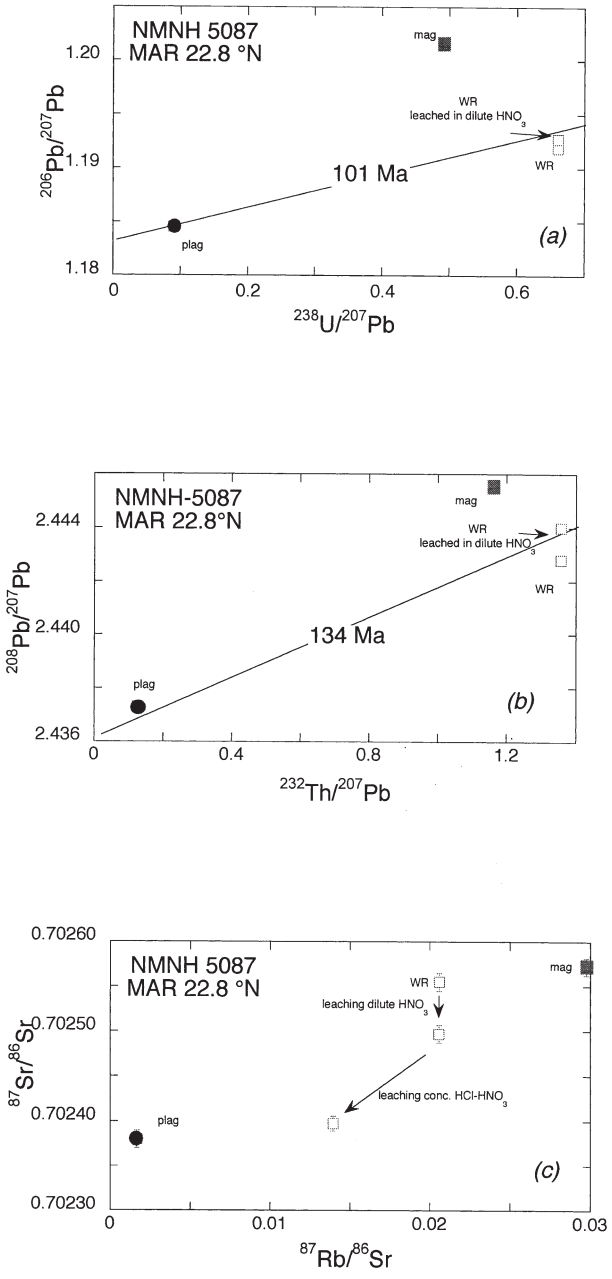

Fig. 4. Pb and Sr isotopic data of mineral fractions and whole rock from sample NM5087, a dredge sample from the Mid-Atlantic Ridge (around 22 °N, see text and Melson et al., 1968, for details). (a) $^{206}Pb/^{207}Pb$ vs. $^{238}U/^{207}Pb$ isochron; (b) $^{208}Pb/^{207}Pb$ vs. $^{232}Th/^{207}Pb$ isochron; (c) $^{87}Sr/^{86}Sr$ vs. $^{87}Rb/^{86}Sr$ isochron diagram. Symbols as defined in Figure 2. Note that extreme leaching removes the $^{87}Sr/^{86}Sr$ variability.

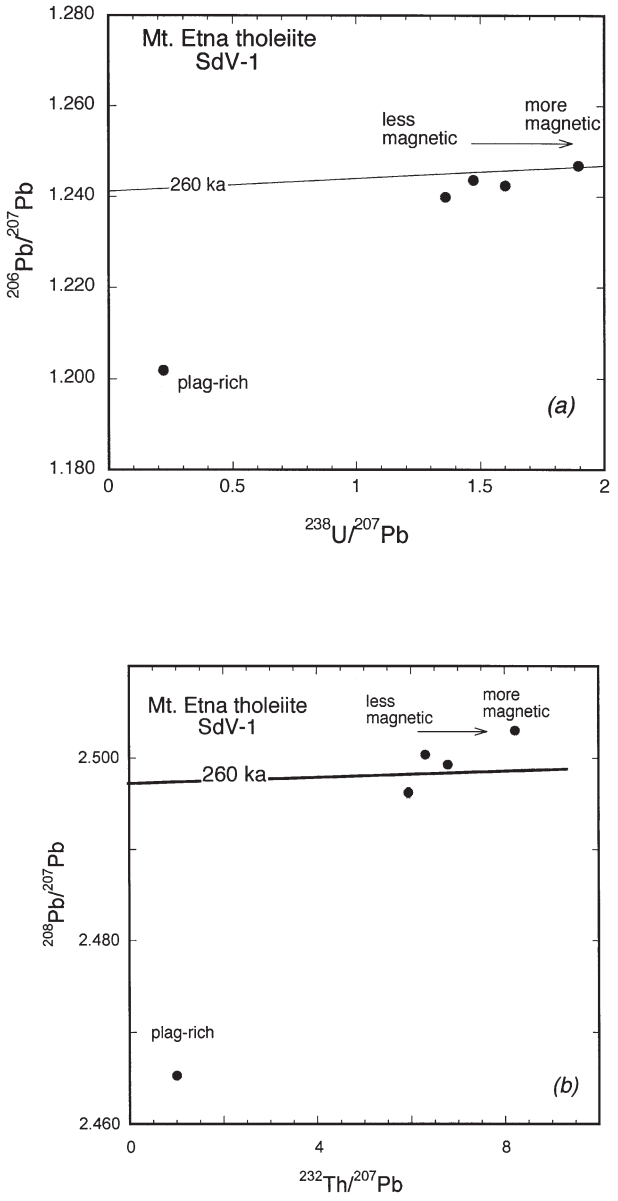

Fig. 5. Magnetic splits from a pre-Etna lava from Stazione di Valcorrente. from the Mid-Atlantic Ridge (around 22 °N, see text and Melson et al., 1968, for details). (a)$^{206}Pb/^{207}Pb$ vs. $^{238}U/^{207}Pb$ isochron; (b) $^{208}Pb/^{207}Pb$ vs. $^{232}Th/^{207}Pb$ isochron; (c) $^{87}Sr/^{86}Sr$ vs. $^{206}Pb/^{207}Pb$ diagram. The low U/Pb and Th/Pb splits (and low $^{206}Pb/^{207}Pb$ and $^{208}Pb/^{207}Pb$) are the least magnetic groundmass/microphenocryst splits, representing the most plag-rich fraction.

in the $^{87}Sr/^{86}Sr$ isotopic ratios among plagioclase, magnetic separates, and WR samples are similar to the range observed for WR samples from the entire Imnaha formation (Hooper and Hawkesworth, 1993). The same is true for both $^{208}Pb/^{207}Pb$ and $^{206}Pb/^{207}Pb$. The isotopic variability of the mineral separates is larger than the range measured in other whole rock samples of the three Rock Creek flows. For the MORB sample, the Pb isotopic variations measured in the mineral separates are greater than the variation seen along the ridge crest, and are about a third of the range seen at 25°N along the Kane Fracture Zone, as shown in Figure 8.

For the Etna sample, the mineral separates show a range of Pb isotopic ratios that is larger than observed for other Etna samples, but similar to the range seen in somewhat older lavas of the nearby Hyblean Plateau (Trua et al., 1998; Fig. 9). The Sr isotopic variations in the Etna sample are small, as are the Sr isotopic variations in the Hyblean lavas and the prehistoric Etna lavas. Cortini and van Calsteren (1985) detected less radiogenic plagioclase feldspars ($^{206}Pb/^{207}Pb \sim 1.22$) and more radiogenic matrix ($^{206}Pb/^{207}Pb \sim 1.25$) in a study of the Mt. Etna lava erupted in 1971. These other observations were made on lavas with considerably larger phenocrysts.

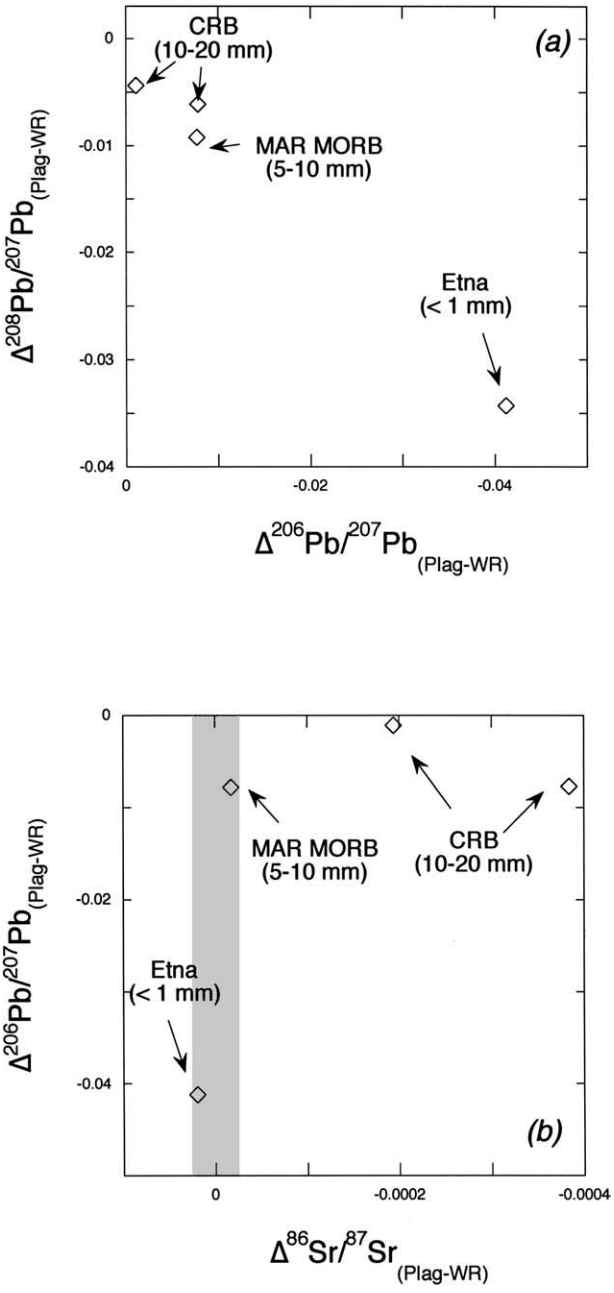

Fig. 6. Variabilities in Pb isotopic signatures in the WR to plagioclase splits. (a) $^{206}Pb/^{207}Pb$ vs. $^{208}Pb/^{207}Pb$; (b) $^{206}Pb/^{207}Pb$ vs. $^{87}Sr/^{86}Sr$.

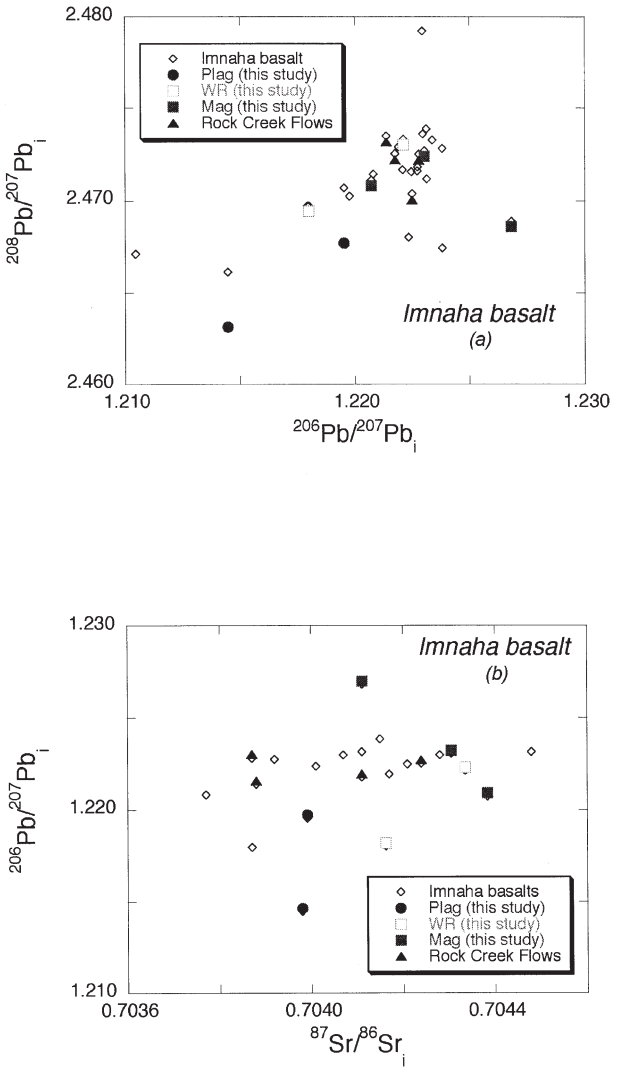

Fig. 7. Regional isotopic data from the CRBG from Hooper and Hawkesworth (1993). Superimposed on the CRBG WR data are the plagioclase, magnetite-rich and WR splits from this study. The data are all normalized to $^{207}Pb/^{204}Pb = 15.49784$. (a) $^{206}Pb/^{207}Pb$ vs. $^{208}Pb/^{207}Pb$; (b) $^{206}Pb/^{207}Pb$ vs. $^{87}Sr/^{86}Sr$.

4.2. Mineral Chemistry and Inclusions

Representative mineral compositions are presented in Table 2. In each sample, there are differences between the early crystallizing plagioclase (i.e., large plagioclase phenocrysts as is the case for the CRBG samples and the MORB, or microphenocrystic cores, as is the case for SdV-1) and the late stage plagioclase (the groundmass phases in the case of the CRBG and the MORB and the feldspar rims in the case of the SdV-1 sample). The feldspar compositional differences in SdV-1 are complemented by differences in the phenocrystic and groundmass olivine compositions.

In the CRBG lavas there are small sulfides throughout the rock. In sample CRB-14, these sulfide grains are a few microns in diameter and are associated with the oxides (predominantly Ti-rich spinels). In CRB-16, there are sulfides included in most of the feldspar phenocrysts. Based on major element analyses, these inclusions are dominantly pyrrhottite. Attempts were made to measure Pb in these sulfides via electron microbeam techniques, but only order of magnitude information is available since the pyrrhotite grains were so small (<5 μm). Lead abundance in the sulfide grains was variable: the Pb contents were above background in each measurement of the sulfide grains, and, the Pb concentrations were as high as 2000 ppm. Based on their size and density, we can compute that a thousand such grains would be required to start to shift Pb isotopic ratios; the inclusions, however, are not that abundant. Sulfides would, of course, have no bearing on the Sr isotopic compositions of the feldspar phenocrysts, since Sr concentrations in feldspar are high (574 and 1029 ppm in the CRB samples).

5. DISCUSSION

The results from both the oceanic and continental basalts indicate that magmas of distinct Pb (and Sr) isotopic composition comingle and mix before eruption. Our proposed model for the generation of the Pb isotopic variations requires mixing at relatively shallow levels. This is especially noteworthy for the MORB sample; our results reinforce recent chemical (e.g., Sours-Page et al., 1999; Coogan et al., 2000) studies which

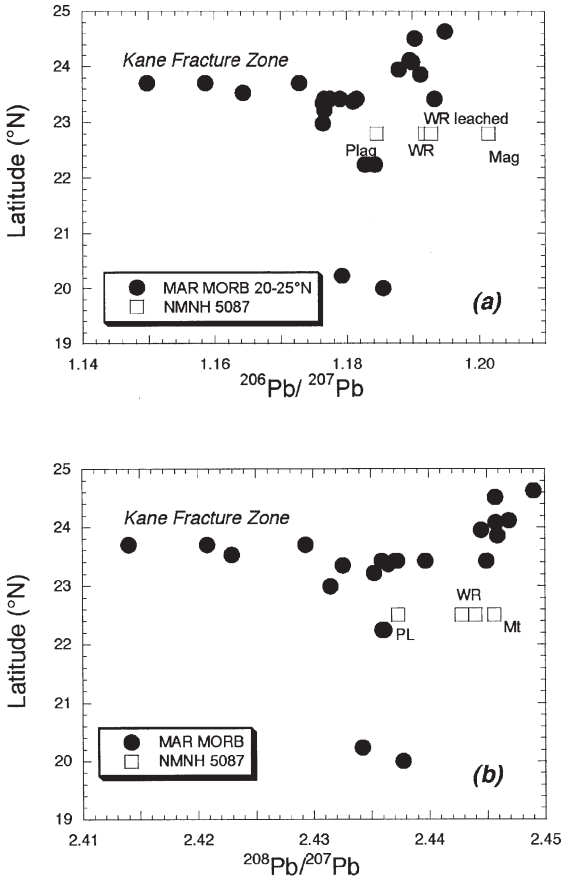

Fig. 8. Regional isotopic data from 19° to 25° N, the Mid-Atlantic Ridge. Data are collected from the PETDB site (available at http://www.ldeo.columbia.edu) and are normalized to $^{207}Pb/^{204}Pb = 15.49784$. Superimposed on regional variations in the MORB WR data are the phase separates from this study.

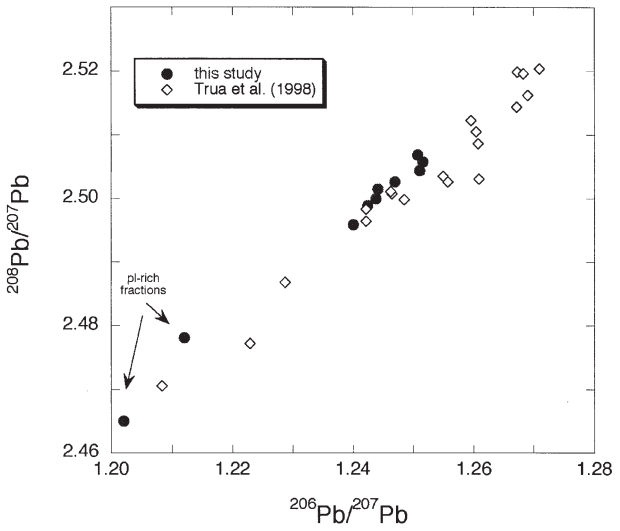

Fig. 9. Regional Pb data from the Mount Etna region in southeastern Sicily. The variable data of the Hyblean plateau demonstrate the isotopic variations that are caused by melting of the Sicilian lithosphere and can be used as a model for formation of plag-WR isotopic disequilibrium by mixing of melts of the lithospheric mantle. The splits of the Etna tholeiite are depicted as filled circles. The Hyblean lavas are tholeiitic and alkaline in composition (data are from Trua et al., 1998). The data are normalized to $^{207}Pb/^{204}Pb = 15.60932$. See text for discussion. The Pb isotopic variability within the Etna sample is similar to that in the suite of lavas from the Hyblean plateau (Pb data are from Trua et al., 1998), which lies <30 km to the SSW of the Etna sample locality. Note that the lavas with the extreme Pb isotopic ratios (one tholeiitic and one alkaline basaltic) were both erupted at 2.03–2.11 Ma ($\pm$0.05, 1); the $^{40}Ar/^{39}Ar$ dates for their eruption are indistinguishable at the 1 σ level (Trua et al., 1997). Sr isotopic data are not presented here since the variations in the SdV sample are indistinguishable at the 2σ level. For comparison to Figures 7 and 8, the Hyblean range in $^{87}Sr/^{86}Sr$ is 0.7028 to 0.7035 (Trua et al., 1998); the ancient Etna magmas bear $^{87}Sr/^{86}Sr$ ranging from 0.7029 to 0.7032 (Giacobbe, 1993; Tanguy et al., 1997; Bryce, 1998).

argue that melt aggregation in MOR systems occurs at crustal levels. Our model begins with a magma that resides in a relatively shallow level magma chamber where plagioclase is crystallizing. A new batch of magma then enters the chamber, mixes with the resident crystal-bearing magma, and is then erupted shortly afterward. The observations require that magmas with different isotopic compositions are stirred together such that the phenocrysts, which presumably come from only one of the magmas, are associated with liquid that is a mixture of both magmas.

5.1. Timescales

This general model of two magmas mixing in a chamber before eruption implies that there are three important timescales. One timescale is provided by the growth of the phenocrysts. The magma source and delivery system must be able to supply magma to the chamber with the observed contrast in isotopic composition within the time it takes to grow the phenocrysts. The time frame associated with magma delivery provides information on the scale of heterogeneity in the magma source. Another timescale is provided by the need to stir together two magmas such that the liquid phase is substantially homogenized, at least over a significant fraction of the volume of the magma chamber. A third timescale arises due to intragranular diffusion. before eruption, the crystals must remain in contact with the mixed liquid for a period that is short relative to the time required to equilibrate crystals and liquid by diffusion.

The timescale for reequilibration of crystals and melt can be calculated using the measured Pb diffusivity in feldspar (Cherniak, 1995) and a diffusion model based on the reequilibration of a spherical crystal in a surrounding matrix of contrasting isotopic composition (Fig. 10; cf. Christensen and DePaolo, 1993, after Carlslaw and Jaeger, 1959). Based on the major element and isotopic compositions of the plagioclase in the pre-Etna tholeiite, we estimate that the maximum degree of

Table 2. Representative phase compositions of phenocrysts, microphenocrysts, and microlites.[a]

Sample name	CRB-16	CRB-16	NM15087	NM15087	SdV-1	SdV-1	SdV-1	SdV-1
Crystal	plag	plag	plag	plag	plag	plag	Ol	Ol
Crystal description	core	rim/coating	phenocryst	rim/groundmass	core	rim/coating	phenocryst	groundmass
No. analyses	82	40	29	12	40	6	9	7
SiO_2 (wt%)	49.13	53.36	46.36	51.84	53.80	57.99	38.56	37.95
Al_2O_3 (wt%)	32.22	28.83	33.79	28.93	29.62	26.04	—	—
FeO (wt%)	0.56	0.59	0.33	0.93	0.63	0.75	20.60	27.58
K_2O (wt%)	0.12	0.30	0.02	0.05	0.05	0.14	—	—
Na_2O (wt%)	2.88	4.80	1.86	4.26	4.62	6.75	—	—
MgO (wt%)	0.11	0.10	0.18	0.42	0.16	0.08	39.80	33.46
CnO (wt%)	14.54	11.24	16.49	12.34	11.90	8.28	0.22	0.42
TiO_3 (wt%)	—	—	—	—	—	—	0.01	0.05
NiO (wt%)	—	—	—	—	—	—	0.22	0.13
Cr_2O_3 (wt%)	—	—	—	—	—	—	0.02	0.03
MnO (wt%)	—	—	—	—	—	—	0.28	0.35
Total	99.56	99.12	99.12	98.89	100.79	100.13	99.70	99.97
An (Mol%)	73	55	83	62	59	40	—	—
Fo (Mol%)	—	—	—	—	—	—	77	68

[a] These compositions are averages of several "spot" analyses on a number of grains. Aside from the spatial variability evident in the differences between core and rim compositions, the crystals were remarkably uniform in composition, with the largest variations formed in the groundmass/rim measurements of the SdV sample, where the 1σ describing the variation of the An and Fo components from the mean was as high as 3%.

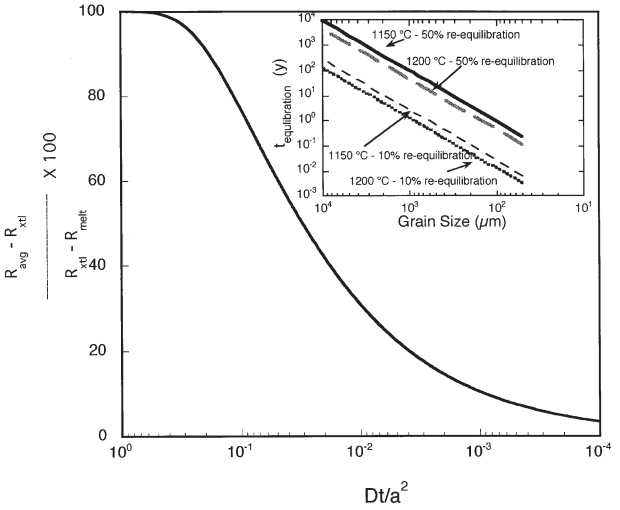

Fig. 10. Reequilibration of crystals in a melt of different isotopic composition (after Christensen and DePaolo, 1993). This calculation is that of a spherical crystal diffusively exchanging with a melt of distinct isotopic composition. The difference between the grain and the liquid is adapted from the mathematical formulations of Carlslaw and Jaeger (1959). A value of 100 on the y-axis indicates that crystals and melts that were once isotopically distinct have returned to isotopic equilibrium. The amount of crystal-melt disequilibrium can be computed using the average composition of the crystal, melt, and the original composition of the crystal. The x-axis represents the product of the diffusivity of the element of interest (D), the time (t) allowed for comingling, and the crystal radius (a). Dta^{-2} can be translated into diffusive timescales for a given reequilibration process using appropriate D data. The figure inset is the computed equilibration time for 10% reequilibration and 50% reequilibration as a function of grain size. The temperature intervals for these calculations were chosen based on the range of liquidus temperatures for plagioclase at low pressures (200–500 Mbar) for the SdV-1 whole-rock composition (Bryce, 1998), as computed using the MELTS algorithm (Ghiorso and Sack, 1995). The diffusion coefficients were computed using the activation energies and D_0 experimentally determined for An_{67} plagioclase by Cherniak (1995).

reequilibration is in the range 10 to 50%, probably closer to the former. This number may also serve as a conservative estimate for the CRBG and MORB samples, based on the size of the isotopic variations observed. In the case of the pre-Etna tholeiite, for 50–100 μm crystals in appropriate temperature intervals, the maximum contact time is days to weeks (inset, Fig. 10). For the CRBG samples and MORB, we estimate the length scale for the feldspar to be ~5 mm (the shortest dimension of the tabular crystals), and the corresponding maximum contact time is 10–100 yr. Our estimate of contact time falls within the range of a recent estimate of magma chamber residence time of 0.1 to 1 kyr based on seismic studies of Axial volcano, near the Juan de Fuca ridge (West et al., 2001). For comparison, our calculated time is considerably shorter than the mingling time of ~550 yr Cooper et al. (2001) suggest for the 1955 Kilauea lava, based on Ra and Th isotopic data.

The mixing time for magmas of basaltic composition can be roughly estimated from fluid dynamical considerations (Kenyon and Turcotte, 1987; Christensen and DePaolo, 1993) using the eddy diffusivity in a turbulently convecting magma. The eddy diffusivity is estimated from:

$$\kappa_{eddy} = 1.34\kappa\left(\frac{Ra}{Ra_{crit}}\right)^{1/3} \quad (4)$$

where Ra is the Rayleigh number describing the convective regime in the magma chamber; Ra_{crit}, the critical Rayleigh number, is ~1700 (cf. Turcotte and Schubert, 1982); and κ, the thermal diffusivity, is approximately 0.001 cm^2/s. The time for mixing the magma (τ_{mix}) is therefore roughly L^2/κ_{eddy}, where L is the maximum dimension of the magma chamber. Substituting parameter values for basaltic magma in a reasonably large (0.1 to 1 km height) chamber with a 50°C temperature difference, yields Ra $\approx 10^{12}$ to 10^{15}, and κ_{eddy} = 3 to 3000 km/yr. If the maximum dimension of the chamber is 10 times the height, the derived timescales are ~0.03 yr for a 1 × 10 km and 0.3 yr for a 0.1 × 1 km chamber. This result suggests that it is possible to mix effectively two basaltic magmas in a time that is comparable to or even significantly shorter than the maximum contact time estimated from intracrystalline diffusion. The values applicable to the Etna tholeiite, where the magma chamber was probably relatively small, would be to the high side of the quoted range and thus marginally problematical.

To approximate the time it takes to grow the feldspar crystals, we assume a growth rate of $\sim 10^{-10}$ cm/s or ~0.03 mm/yr (cf. Resmini and Marsh, 1995). Hence the large crystals in the CRB and MORB samples might have taken 300 yr to grow, whereas the Etna feldspars would have required only ~3 yr. The crystal growth timescale is therefore significantly longer than the timescales suggested for either mixing or intracrystalline diffusion.

The estimated timescales indicate that it is possible to grow crystals in a magma chamber, add magma of another composition, mix the two magmas together and erupt them while preserving the isotopic identity of the first magma in the entrained crystals. The timescale for mixing and eruption is quite short, weeks to months, so it is possible to retain the isotopic distinctiveness of quite small feldspar phenocrysts. Plagioclase of labradorite composition is also nearly neutrally buoyant in a basalt liquid, hence the crystals could be easily mobilized during recharge events and/or they could be mixed and suspended in a vigorously convecting magma during the short time required to mix the magmas.

Evidence of rapid magma mixing is also provided by the populations of plagioclase feldspar ([An] > $\sim An_{70}$, [An] $\sim An_{60}$, [An] < $\sim An_{55}$) in each of the Imnaha basalts. The largest plagioclase crystals are the most An-rich (>An_{70}) followed by smaller phenocrysts ($\sim An_{60-70}$) and the groundmass phases and rimming plagioclase ($\sim An_{55}$). Sample NMNH 5087 also has evident compositional differences between plagioclase core, rim and groundmass crystals (Table 2). The pre-Etna tholeiite has quite homogeneous compositions in the cores of the microphenocrysts ($\sim An_{55-60}$). Most of these cores were then coated by plagioclase of much lower An content ($\sim An_{30-40}$). The coat is approximately 10 μm thick (Fig. 11), which can be added to the existing feldspar grains on a timescale of about a few months at the above-quoted crystal growth rates. Changing P_{H_2O} in the magma could influence and increase the crystallization rate (cf. Kuritani, 1999). Such a shift, coupled with the changing temperature and pressure conditions associated with the final stages of ascent and eruption, could

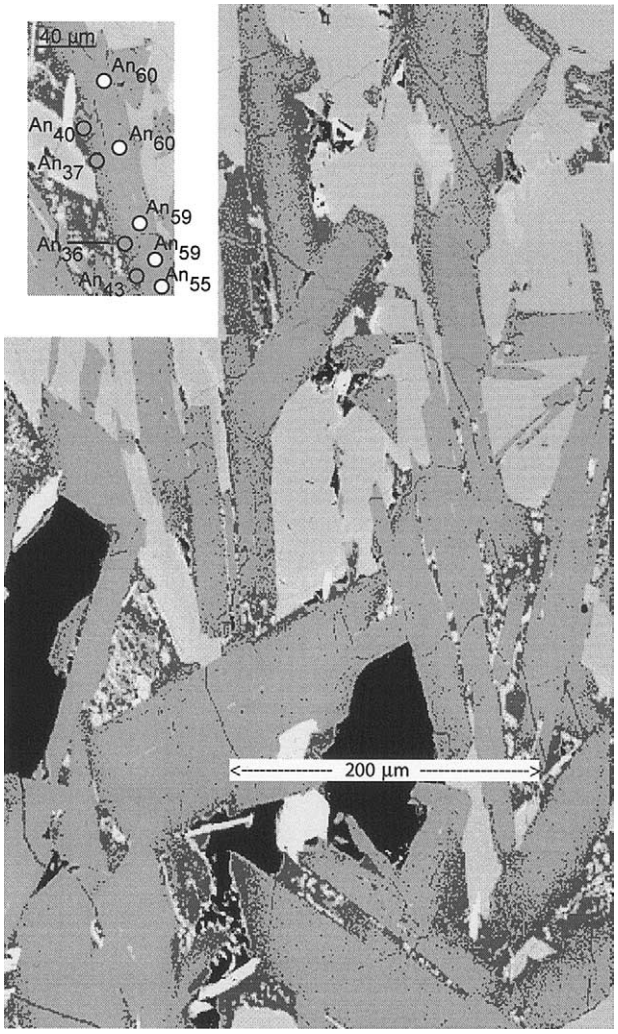

Fig. 11. Enhanced high-magnification BSE images of the groundmass from the SdV-1 sample. Brighter colors (white > light gray > dark gray) indicate higher average molecular weight. Note the dark gray rims of many of the plagioclase laths, corresponding to lower An contents in the feldspars. An example of plagioclase composition for one such area is shown in the inset.

also produce variations in feldspar composition. An example of syn-eruptive feldspar crystallization can be found in an alkali basalt from Rishiri volcano (Japan) where Kuritani (1999) documents ~ a 6 mol% An content difference between the rim and the crystal interior. This difference is much smaller than that which we see in our samples (up to ~20 mol% An), suggesting that for our samples different magma compositions are probably required.

5.2. Assimilation of Crustal Materials

Assimilation of crustal materials could also cause gradual changes in the isotopic composition of magmas in crustal chambers. Early formed plagioclase, for instance, could fail to reequilibrate isotopically with a magma that is shifting in isotopic composition due to addition of an assimilant. Several aspects of the data, however, indicate that the observed variations are probably not due to assimilation. Recent studies have shown that wallrock assimilation in shallow crustal basaltic magma chambers is typically minimal (e.g., Stewart and DePaolo, 1990,1996). The Pb isotopic variations we have observed are quite large to be accommodated by assimilation, and, although there has been a proposal to the contrary by Edwards and Russell (1998), the timescales for assimilation might be long. A more recent study by Kent et al. (2002) of melt inclusions from Yemeni basalts related to continental flood volcanism indicate that crustal assimilation can take place at alarming rates, perhaps at levels where the mass assimilated is much greater than the mass crystallized. Such assimilation, however, seems to be volumetrically insignificant for the Yemeni samples for two reasons: (1) the suite of whole rock hosts for these apparently contaminated melt inclusions showed no signs of assimilation (Hf and Nd isotopic compositions are strongly correlated in these samples, a trend which would not be expected with large amounts of assimilation) and (2) the host phase for these melt inclusions is Fo-rich olivine ($Fo_{85–90}$). We offer here arguments that assimilation is not the most likely explanation of the isotopic variations we measured, but, we cannot prove that it has not played a role in some of the samples.

A study conducted on the Imnaha group Rock Creek basalt flows (Chesley and Ruiz, 1998) found that these two flows (the RC1 and RC2 flows) had, by a large amount, the least radiogenic Os isotopic signatures of all the CRBG lavas studied. Although this does not rule out contamination, it suggests that there has been very little crustal material added to the magmas. As a part of their study, Chesley and Ruiz conducted a detailed study of Re-Os isotopic and elemental signatures of mineral separates from the RC2 flow and could show no statistically significant difference between the magnetic separates and the nonmagnetic fractions (plagioclase/etc.). Further evidence against crustal assimilation sensu stricto comes from our isotopic data for the mineral separates for both samples. The Nd isotopic composition of the plagioclase in CRB-16 is approximately 2 ε units lower than that of the other phases in this rock (Table 1). Incorporation of crustal materials would generally lower the ε_{Nd}, but it would also increase the Sr isotopic signature to more radiogenic $^{87}Sr/^{86}Sr$ values. The CRB-16 sample bears plagioclase with a lower ε_{Nd}, but, interestingly, the same plagioclase split has the lowest $^{87}Sr/^{86}Sr$ in the rock. These data, coupled with the plumelike $^{3}He/^{4}He$ value for the CRB-14 of Dodson et al. (1997) strongly suggest that the isotopic variability in the Imnaha samples is mantle-derived.

Assimilation of crustal materials also cannot readily explain the observed Pb isotopic variations in NMNH 5087. Pb isotopic compositions of modern-day Fe-Mn crusts from the Atlantic seamounts (Abouchami et al., 1999; Burton et al., 1997) can be used as a proxy for the Pb isotopic composition of Atlantic seawater ($^{206}Pb/^{204}Pb \sim 19$, $^{207}Pb/^{204}Pb \sim 15.7$; $^{208}Pb/^{204}Pb \sim 39.0$). Hence an appropriately normalized $^{206}Pb/^{207}Pb$ value of the seawater is ~1.21, and an appropriately normalized $^{208}Pb/^{207}Pb$ value is ~2.50. Assimilation of previously-altered basalt could shift the Pb isotopic compositions in the right direction; however, a change in $^{206}Pb/^{207}Pb$ from the plagioclase value to that of the whole rock would require assimilation of an amount of Pb equal to at least 50% of the Pb originally in the magma. The resulting $^{208}Pb/^{207}Pb$ isotopic signature of

such a mixture is >2.46–2.47, considerably higher than that observed for either the magnetic fraction or the whole rock for the NMNH sample. A similar mass balance argument may be made for the Pb and Sr isotopic compositions of the plagioclase and whole-rock of NMNH-5087. Assimilation of sufficient seawater, brine material (cf. Kent et al., 1999) or seawater-altered material to explain the heterogeneity in Pb isotopic compositions would produce too radiogenic a Sr isotopic signature in the WR. Thus, seawater, seawater- or hydrothermally altered basalt seem unlikely candidates for an assimilant.

An appropriate assimilant for the SdV-1 sample must be able to shift the Pb isotopic composition by a large amount (3% in $^{206}Pb/^{207}Pb$) without changing the Sr isotopic composition significantly. Interestingly, both the SdV sample that we have studied here and the 1971 lava studied by Cortini and van Calsteren (1985) contain plagioclase with lower $^{206}Pb/^{207}Pb$ and lower $^{208}Pb/^{207}Pb$ than the WR and, as well, plagioclase-WR splits that do not have significantly different $^{87}Sr/^{86}Sr$. Although oxygen data for the Stazione di Valcorrente samples are not available, whole rock $\delta^{18}O$ values for the prehistoric Mt. Etna tholeiites and lava from the 1971 Etna eruption fall within the normal mantle range (5.4 ± 0.3‰ with 0.2‰ analytical precision, Marty et al., 1994). The 1971 eruption predates the Etna lavas which bear strong signatures of assimilation and fractional crystallization (AFC) processing (Clocchiatti et al., 1986; Giacobbe, 1993), namely alkali enrichment with increasingly radiogenic $^{87}Sr/^{86}Sr$. The lavas from the 1971 eruption fall in the relatively high-MgO field of Etna lavas (>6 wt%) and have a $^{3}He/^{4}He$ signal that is associated with mantle-derived materials (Marty et al., 1994). The lack of change in $\delta^{18}O$ among the prehistoric Etna lavas, coupled with the constant $^{87}Sr/^{86}Sr$ in these samples, suggests that assimilation of crustal materials does not play a significant role in the generation of these lavas.

5.3. Implications for Magma Transport, Supply, and Source Heterogeneity

5.3.1. Source heterogeneities

Overall, the isotopic variations that we observe within crystals in single samples of basalt are similar to or somewhat smaller in magnitude than the variations in whole rock samples from the region erupted at about the same time. The values we measure for $^{206}Pb/^{207}Pb$, $^{208}Pb/^{207}Pb$ and $^{87}Sr/^{86}Sr$ are also within the range measured for whole rocks. We infer therefore that the isotopic variations we observe are indicative of the isotopic heterogeneity in the basalt magma sources. The fact that these heterogeneities are evident in phenocrysts in a single basalt flow gives some information on the size of the heterogeneities in the mantle.

A simple way of looking at the preservation of the isotopic heterogeneity in basalts is in terms of the thickness of the melting region (Δz), the mantle upwelling rate (W) that is generating decompression melting, the melt velocity relative to the matrix (w), and the hydrodynamic dispersion coefficient, D_h, that characterizes the flow of melt through the melting region (DePaolo, 1996; Hauri, 1997). Any isotopic variations arranged vertically in the upwelling mantle source material will be seen in the lavas, but with decreased amplitude. The timescale (τ) over with which these variations occur is related to the vertical length of the heterogeneity (L) by $\tau = L/W$. The amplitude of the isotopic variations, however, is decreased relative to what is present in the mantle by a factor that depends on the melt zone dispersion coefficient and other factors:

$$A = A_0 \exp\left(\frac{-4\pi^2 D_h \Delta z}{w_i^3 \tau^2}\right) \quad (5)$$

where A_0 is the amplitude of the isotopic variation in the mantle source, A is the amplitude as delivered to the crustal magma chamber, and w_i is the velocity with which the particular element is transported through the melting region, which for incompatible elements is slightly smaller than the actual melt velocity as a result of retardation (Albarède, 1992; DePaolo, 1996).

The length scale of the isotopic heterogeneities needed to satisfy the observations, can be calculated from the timescale of crystal growth, which for the MORB and CRB samples is roughly 1000 yr. Current models estimate that the thickness of the melting region beneath MOR is variable but might range up to a maximum of 30 km right under the ridge axis, and the upwelling rate is similar to the seafloor spreading velocity of ca. 5 cm/yr (cf. Kelemen et al., 1997, for review). At a velocity of 5 cm/yr, the scale of the heterogeneities is calculated to be 5000 cm or 50 m. For the CRB, the upwelling rate could be somewhat higher, so the scale of the heterogeneity could be hundreds of meters. These numbers are not precise, but the significant point is that they are much smaller than the length of ridge (500 km) over which similar magnitude variations are observed in MORB whole rock samples (Fig. 8).

Another significant aspect of the data is that the amplitude of the variations in the phenocrysts is not much smaller than the range observed in whole rocks. This means that the absolute value of the argument on the exponential term in Eqn. 5 is order unity (or smaller) if the whole rocks represent the actual amplitudes in the mantle. Assuming that $A/A_0 = e^{-1}$, and setting Δz at 10 km for MORB (a mean value), and $w_i = 50$ cm/yr yields an estimate of the dispersivity of ~0.6 m. Increasing the melt velocity or decreasing the melt zone thickness would increase the calculated dispersivity, but for any set of parameter values the calculated dispersivity is very small. One way to interpret the small value is that melt moves by porous, grain scale flow and hence there is little vertical mixing in the melt column. Another option is that the actual amplitudes of the isotopic variations in the mantle source material are much larger than the range observed in whole rocks. This latter inference would seem to be consistent with the large isotopic variations observed in some melt and mineral inclusions in olivine from other settings (e.g., Eiler et al., 1998; Saal et al., 1998). For the Etna tholeiite sample, the inferred timescale for crystal growth is much shorter (10 yr as opposed to 10^3 yr); adjusting the mantle upwelling and melt migration velocity to smaller values predicts the calculated size of the heterogeneity to be much smaller (<10 m) and the dispersivity would need to be small as well.

A more general model would allow for both horizontal and vertical heterogeneities. In this case, regardless of the timescale, to supply melts of more than one isotopic composition at about the same time, the heterogeneities would need only to

have a length scale that is smaller than the horizontal dimension of the melting region feeding the volcano or ridge segment. In this model it might be possible to have the heterogeneity scale be as large as several kilometers, and there would be no constraint on melt zone dispersivity.

The length scales of mantle heterogeneities have been investigated for quite some time (see Zindler and Hart, 1986, for a comprehensive review). In this study we have observed $\Delta^{206}Pb/^{207}Pb = {}^{206}Pb/^{207}Pb_{hi} - {}^{206}Pb/^{207}Pb_{lo}$ of ~0.02 to 0.05 in individual samples. This value comprises around 10 to 25% of the variability in the mantle worldwide (the worldwide $\Delta^{206}Pb/^{207}Pb$ is ~0.19). In comparison, the worldwide range of $^{208}Pb/^{207}Pb$ is smaller ($\Delta^{208}Pb/^{207}Pb \sim 0.1$), but our samples individually document a $\Delta^{208}Pb/^{207}Pb$ that again accounts for approximately 10 to 25% of this worldwide variation. Our data set is particularly well suited to such analyses of heterogeneities as these samples likely represent degrees of melt smaller than those encountered during MORB petrogenesis (see, e.g., McKenzie and Bickle, 1988, vs. Kelemen et al., 1997). Zindler et al. (1984) identify the relatively large degrees of melting associated with MORB petrogenesis as a handicap for using MORBs to evaluate the scale of spatial heterogeneity, suggesting that the chemical differences of MORBs may reflect differences in the melting process.

In a later study, Reisberg and Zindler (1986) document comparable and even larger scales of mantle heterogeneities in the Ronda ultramafic complex that occur over length scales similar to those we compute above (10s to 100s of meters). There are always concerns associated with the use of ultramafic bodies emplaced on continents to gain information about the melting region of the mantle. One, as Reisberg and Zindler (1986) identify, is establishing with certainty a mantle origin of these ultramafic bodies. Even accepting origin in the mantle, there still remain questions regarding whether the compositional heterogeneities are undeniably relics of inhomogeneities that were once in the mantle as opposed to artifacts of high temperature processes associated with the emplacement of these lithologies onto continental crust. The good agreement of our approximation of spatial heterogeneities with this and other ultramafic studies (e.g., Polve and Allegre, 1980) provides another line of evidence that the heterogeneities observed in these ultramafic bodies do indeed place constraints on the sizes of mantle heterogeneities.

5.3.2. *Heterogeneities introduced during transport*

It is also possible that the isotopic variations are introduced during the magma migration process. This may be important in the magmas that travel through the subcontinental lithosphere before they are erupted. Recent numerical models by Spiegelman and Kelemen (2003) document that reactive transport coupled with channelized flow can generate large differences in melt composition. These models, even in the case of a homogeneous two-phase (pyroxene-olivine) mantle, can produce up to seven orders of magnitude variation in the abundance of the least compatible trace elements. In the case of the continental lithosphere, where, over long periods of time, mantle may be metasomatically enriched and tectonically isolated from rehomogenization via mantle convection, such selective dissolution of mantle phases, in particular pyroxene, could have isotopic consequences for the signatures of migrating melt.

A detailed Sr, Pb, and Os isotopic study by Carignan et al. (1996) of mantle xenoliths harvested from the Quaternary basalts of the Alligator lake volcanic center in the Yukon provides some support for this argument. This suite of spinel-lherzolites has $^{206}Pb/^{207}Pb$ ranging from 1.19 to 1.23 and $^{208}Pb/^{207}Pb$ ranging from 2.44 to 2.48. There are no major Sr isotopic differences between the cpx splits and the whole rock. As we see in our study of basaltic phenocrysts, the Pb isotopic differences in minerals from one xenolith have the same sort of isotopic spread evident in the whole suite, with olivine and orthopyroxene having the least radiogenic $^{206}Pb/^{207}Pb$ and $^{208}Pb/^{207}Pb$. Clinopyroxene crystals from these xenoliths contain the most Pb and bear the most radiogenic Pb isotopic signatures. Carignan et al. (1996) argue that cpx in particular shows a marked contrast in U and Pb content based upon metasomatism, thus, arguing that cpx "scavenges" U and Pb from metasomatic fluids. Although these xenoliths are most likely plucked from the walls of the dike formed as the magma ascends via crack flow (cf. Shaw, 1980), it is reasonable to assume that the mantle below this transition also bears heterogeneities on comparable length scales.

Using these signatures, we can consider the isotopic consequences of reactive transport in such a lithospheric mantle. Magma transported via porous flow accompanied by orthopyroxene dissolution (e.g., Wagner and Grove, 1998) may inherit less radiogenic $^{206}Pb/^{207}Pb$ and $^{208}Pb/^{207}Pb$, whereas magma ascending via reactive transport in a channelized flow forming as a consequence of clinopyroxene reaction may tend to inherit a component with a more radiogenic $^{206}Pb/^{207}Pb$ and $^{208}Pb/^{207}Pb$ signature. This metasomatic enrichment does not affect the Sr isotopes as the Sr isotopic compositions of the phases of the Alligator Lake xenoliths are relatively homogeneous. The metasomatic enrichment may also not manifest itself in the He isotopic signal of the resultant magma if high ^{3}He signatures are derived from sublithospheric sources during the magma generation process or if there is a net ^{3}He flux to the lithosphere from sublithospheric sources, perhaps by CO_2-rich fluids as hypothesized by Gautheron and Moreira (2002) to reconcile the higher-than expected $^{3}He/^{4}He$ signatures of lithospheric mantle xenoliths with the known U concentrations of lithosphere.

The Yukon xenolith suite is perhaps an extreme case of Pb isotopic variability, one that is preserved since the last metasomatic event happened ~30 Ma (Carignan et al., 1996). Yet even for lithospheric mantle held at higher temperatures, containing metasomatically enriched pyroxene (either by fluids or silicate magmas stalling out in a peridotite and forming wehrlite, e.g., Xu et al., 1996), it is interesting to note that the diffusive reequilibration timescales are long. To compute the diffusive reequilibration time (τ_{DR}) for orthopyroxene at mantle temperatures (1100°C), we can use the same we used to compute the τ_{DR} for plagioclase crystals in magma chambers (cf. Fig. 10). Using the appropriate diffusivity data (Cherniak, 1998, 2001), we find that only fifty percent of a distinct Pb isotopic signature in a 5 mm orthopyroxene crystal would diffuse away in 0.75 Myr. The τ_{DR} for a similarly sized clinopyroxene crystal is shorter by about a factor of 5. These τ_{DR}'s are computed based on 1-atm diffusivity data; we are not aware of laboratory measurements of activation volume for Pb

diffusion in orthopyroxene or clinopyroxene, but if the sensitivity of Pb diffusion to pressure is as high as that of REE diffusion in pyroxene (cf. van Orman et al., 2002), this timescale for diffusive equilibration could be as long as several million years. For comparison, van Orman et al. (2002) find a diffusive equilibration time for Nd to be on the order of 1 Gy in lithospheric mantle at 1.5 GPa and 1150°C. Given the isotopic signature of phases from mantle xenoliths and long reequilibration times, it is feasible that enrichments from earlier metasomatic events could be "stored" in the lithospheric mantle in clinopyroxene-rich rocks and then later sampled by migrating magmas. Thus, magmas could inherit their isotopic compositions from the source that directly melted to form them or via transport in the lithosphere.

6. CONCLUSIONS AND IMPLICATIONS

We have reported first results of an application of a high resolution Pb isotopic petrogenetic tracer for basalts, based on normalization to $^{207}Pb/^{204}Pb$ as introduced by Getty and DePaolo (1995). Each basalt sample studied has initial Pb isotopic disequilibrium, especially in plagioclase feldspar phenocrysts relative to whole rock or matrix samples. Basaltic samples from the CRBG also demonstrate Sr isotopic heterogeneity in the phenocrysts. The Pb isotopic variability is interpreted in terms of a model where crystal-bearing magma resident in a shallow chamber is mixed with magma of distinct isotopic composition just before eruption. This type of isotopic effect has been documented previously for more silica-rich magma types, but there are few previously reported examples for basalt.

The observed magnitude of the Pb (and in one case Sr and Nd) isotopic differences between crystals and groundmass is roughly 30 to 80% of the variability observed in whole rock samples of regional lavas erupted at about the same time (within a few hundred thousand years) from the local area (within 30–300 km). The fact that such a large amount of the regional heterogeneity can be found in single samples of basalt lava suggests that the length scale of heterogeneities in the mantle sources are quite short—less than hundreds of meters if arranged vertically and less than several kilometers if arranged horizontally. Our observations also require that the heterogeneities are not attenuated by mixing during transport through the melting region, or that the mantle heterogeneities have a much larger amplitude than is evident from whole rock samples taken from a relatively wide area. In the case of the MORB sample we have studied from the mid-Atlantic Ridge, the heterogeneities present on scales of tenths to several km in the source region of the lava we studied, must be about as large in isotopic contrast as those present along a 500 km segment of the ridge.

The present results appear to be in concert with recent reports of large isotopic and trace element variations in melt inclusions in olivine phenocrysts (Eiler et al., 1998; Saal et al., 1998; Rose et al., 2001). The existence of large amplitude isotopic heterogeneities in the mantle on short length scales strongly suggests that isotopic heterogeneities in the mantle are not efficiently homogenized by mantle convection in the time available between their introduction and the sampling by subsequent magma generation processes (Carlson, 1984; Gautheron and Moreira, 2002; Stewart and DePaolo, 1996; Getty and DePaolo, 2000; Van Orman et al., 2002).

Acknowledgments—We gratefully acknowledge W. Melson and the Division of Petrology and Volcanology, Department of Mineral Sciences, Smithsonian Institution for providing the sample from 22.8°N. Thanks are also due to Jo C. Lin, Tom Owens and John Donovan for help with some of the analytical and technical work. We also thank J. Davidson, S. Galer, D. Graham, M. Thirlwall and an anonymous referee for their helpful and constructive reviews. Support for this study was provided by the National Science Foundation (EAR-9909590). Support for laboratory operations was also provided by the Director, Office of Energy Research, Basic Energy Sciences, Chemical Sciences, Geosciences and Biosciences Division of the U.S. Department of Energy under Contract No. De-AC03-76SF00098.

Associate editor: S. J. G. Galer

REFERENCES

Abouchami W., Galer S. J .G., and Koschinsky A. (1999) Pb and Nd isotopes in NE Atlantic Fe-Mn crusts: Proxies for trace metal paleosources and paleocean circulation. *Geochim. Cosmochim. Acta* **63,** 1489–1505.

Albarède F. (1992) Residence time analysis of geochemical fluctuations in volcanic series. *Geochim. Cosmochim. Acta* **67,** 615–621.

Baksi A. K. (1989) Re-evaluation of the timing and duration of the extrusion of the Imnaha, Picture Gorge, and Grand Ronde Basalts, Columbia River Basalt Group. In *Volcanism and Tectonism in the Columbia River Flood-Basalt Province* (eds. S.P. Reidel and P.R. Hooper). pp 105–112, Geological Society of America Special Paper 239.

Bryce J. G. (1998) Aspects of alkaline and basaltic magmagenesis. Ph.D. thesis. University of California, Santa Barbara.

Burton K. W., Ling H. F., and O'Nions R. L. (1997) Closure of the Central American Isthmus and its impact on North Atlantic Deep Water Circulation. *Nature* **386,** 382–385.

Carlslaw H. S. and Jaeger J. C. (1959) Conduction of Heat in Solids 2nd ed. Clarendon Press.

Carlson R. W. (1984) Isotopic constraints on Columbia River flood basalt genesis and the nature of the subcontinental mantle. *Geochim. Cosmochim. Acta* **48,** 2357–2372.

Carignan J., Ludden J., and Francis D. (1996) On the recent enrichment of subcontinental lithosphere: A detailed U-Pb study of spinel lherzolite xenoliths, Yukon, Canada. *Geochim. Cosmochim. Acta* **60,** 4241–4252.

Cherniak D. J. (1995) Diffusion of lead in plagioclase and K-feldspar: An investigation using Rutherford Backscattering and resonant nuclear reaction analysis. *Contrib. Mineral. Petrol.* **120,** 358–371.

Cherniak D. J. (1998) Pb diffusion in clinopyroxene. *Chem. Geol.* **150,** 105–117.

Cherniak D. J. (2001) Pb diffusion in Cr diopside, augite, and enstatite, and consideration of the dependence of cation diffusion in pyroxene on oxygen fugacity. *Chem. Geol.* **177,** 381–397.

Chesley J. T. and Ruiz J. (1998) Crust-mantle interaction in large igneous provinces: Implications from the Re-Os systematics of the Columbia River flood basalts. *Earth Planet. Sci. Lett.* **154,** 1–11.

Christensen J. N. and DePaolo D. J. (1993) Time scales of large volume silicic magma systems: Sr isotopic systematics of phenocrysts and glass from the Bishop Tuff, Long Valley, California. *Contrib. Mineral. Petrol.* **113,** 100–114.

Clocchiatti R., Joron J.-L., and Treuil M. (1986) The role of selective alkali contamination in the evolution of recent historic lavas of Mt. *Etna. Bull. Volc. Geotherm. Res.* **34,** 241–249.

Coogan L. A., Kempton P. D., Saunders A. D., and Norry M. J. (2000) Melt aggregation within the crust beneath the Mid-Atlantic Ridge: Evidence from plagioclase and clinopyroxene major and trace element compositions. *Earth Planet. Sci. Lett.* **176,** 245–257.

Cooper K. M., Reid M. R., Murrell M. T., and Clague D. A. (2001) Crystal and magma residence at Kilauea Volcano, Hawaii: ^{230}Th-^{226}Ra dating of the 1955 east rift eruption. *Earth Planet. Sci. Lett.* **184,** 703–718.

Cortini M. and van Calsteren P. W. C. (1985) Lead isotope differences between whole-rock and phenocrysts in recent lavas from southern Italy. *Nature* **314,** 343–345.

Davidson J. P. and Tepley F. J. (1997) Recharge in volcanic systems: Evidence from isotope profiles of phenocrysts. *Science* **275,** 826–829.

Davidson J., Tepley F., III, Palacz Z., and Meffan-Main S. (2001) Magma recharge, contamination and residence times revealed by in situ laser ablation isotopic analysis of feldspar in volcanic rocks. *Earth Planet. Sci. Lett.* **184,** 427–442.

DePaolo D. J. (1978) Study of magma sources, mantle structure and the differentiation of the earth using variations of $^{143}Nd/^{144}Nd$ in igneous rocks. Ph.D. thesis. California Institute of Technology.

DePaolo D. J. (1996) High-frequency isotopic variations in the Mauna Kea tholeiitic basalt sequence: Melt zone dispersivity and chromatography. *J. Geophys. Res.* **101,** 11855–11864.

DePaolo D. J., Bryce J. G., Dodson A., Shuster D. L., and Kennedy B. M. (2001) Isotopic evolution of Mauna Loa and the chemical structure of the Hawaiian plume. *Geochem. Geophys. Geosyst.* **2**, Paper number 2000GC000139.

Dickin A. P. (1995) Radiogenic Isotope Geology. Cambridge University Press.

Dodson A., Kennedy B. M., and DePaolo D. J. (1997) Helium and neon isotopes in the Imnaha Basalt, Columbia River Basalt Group: Evidence for a Yellowstone plume source. *Earth Planet. Sci. Lett.* **150,** 443–451.

Edwards B. R. and Russell J. K. (1998) Time scales of magmatic processes: New insights from dynamic models for magmatic assimilation. *Geology* **26,** 1103–1106.

Eiler J. M., McInnes B., Valley J. W., Graham C. M., and Stolper E. M. (1998) Oxygen isotope evidence for slab-derived fluids in the subarc mantle. *Nature* **393,** 777–781.

Gautheron C. and Moreira M. (2002) Helium signature of the subcontinental lithospheric mantle. *Earth Planet. Sci. Lett.* **199,** 39–47.

Getty S. J. and DePaolo D. J. (1995) Quaternary geochronology by the U-Th-Pb method. *Geochim. Cosmochim. Acta* **59,** 3267–3272.

Getty S. J. and DePaolo D. J. (2000) U-Pb and Th-Pb geochronology in Quaternary rocks. In *Quaternary Geochronology: Methods and Applications* (eds. J.S. Noller, J.M. Sowers, and W.R. Lettis). pp. 121–129. AGU Reference Shelf Series Vol. 4.

Ghiorso M. S. and Sack R. O. (1995) Chemical mass transfer in magmatic processes IV: A revised and internally consistent thermodynamic model for the interpolation and extrapolation of liquid-solid equilibria in magmatic systems at elevated temperatures and pressures. *Contrib. Mineral. Petrol.* **119,** 197–212.

Giacobbe A. (1993) An integrated petrologic, petrochemical and isotopic study of Mount Etna lavas: 300,000 years of volcanic history. M.A. thesis. University of California, Santa Barbara.

Gillot P. Y., Kieffer G., and Romano R. (1994) The evolution of Mount Etna in light of potassium-argon dating. *Acta Vulcanol.* **5,** 81–87.

Gautheron C. and Moreira M. (2002) Helium signature of the subcontinental lithospheric mantle. *Earth Planet. Sci. Lett.* **199,** 39–47.

Hauri E. H. (1997) Melt migration and mantle chromatography, 1: Simplified theory and conditions for chemical and isotopic decoupling. Earth Planet. Sci. Lett. **153**, 1–19.

Hawkesworth C. J., Blake S., Evans P., Hughes R., Macdonald R., Thomas L. E., Turner S. P., and Zellmer G. (2000) Time scales of crystal fractionation in magma chambers—Integrating physical, isotopic and geochemical perspectives. *J. Petrol.* **41,** 991–1006.

Hooper P. R., Kleck W. D., Knowles C. R., Reidel S. P., and Thiessen R. L. (1984) The Imnaha Basalt, Columbia River Basalt Group. *J. Petrol.* **25,** 473–500.

Hooper P. R. and Hawkesworth C. J. (1993) Isotopic and geochemical constraints on the origin and evolution of the Columbia River basalt. *J. Petrol.* **34,** 1203–1246.

Hooper P. R., Binger G. B., and Lees K. R. (2002) Age of the Steens and Columbia River flood basalts and their relationship to extension-related calc-alkalic volcanism in eastern Oregon. *Geol. Soc. Am. Bull.* **114,** 43–50.

Kelemen P. B., Hirth G., Shimizu N., Spiegelman M., and Dick H. J. B. (1997) A review of melt migration processes in the adiabatically upwelling mantle beneath oceanic spreading ridges. *Phil. Trans. R. Soc. Lond. A* **355,** 283–318.

Kent A. J. R., Clague D. A., Honda M., Stolper E. M., Hutcheon I. A., and Norman M. D. (1999) Widespread assimilation of a seawater-derived component at Loihi Seamount, Hawaii. *Geochim. Cosmochim. Acta* **63,** 2749–2761.

Kent A. J. R., Baker J. A., and Wiedenbeck M. (2002) Contamination and melt aggregation processes in continental flood basalts: Constraints from melt inclusions in Oligocene basalts from Yemen. *Earth Planet Sci. Lett.* **202,** 577–594.

Kenyon P. M. and Turcotte D. L. (1987) Along-strike magma mixing beneath mid-ocean ridges: Effects on isotopic ratios. *Earth Planet. Sci. Lett.* **84,** 393–405.

Kistler R. W. and Peterman Z. E. (1978) Reconstruction of crustal blocks of California on the basis of initial strontium isotopic compositions of Mesozoic granitic rocks. Prof. Paper 1071. U.S. Geological Survey.

Knesel K. M., Davidson J. P., and Duffield W. A. (1999) Evolution of silicic magma through assimilation and subsequent recharge: Evidence from Sr isotopes in sanidine phenocrysts, Taylor Creek Rhyolite, NM. *J. Petrol.* **40,** 773–786.

Kuritani T. (1999) Phenocryst crystallization during ascent of alkali basalt magma at Rishiri volcano, northern Japan. *J. Volcanol. Geotherm. Res.* **88,** 77–97.

Luo X., Rehnkämper M., Lee D. C., and Halliday A. N. (1997) High precision $^{230}Th/^{232}Th$ and $^{234}U/^{238}U$ measurements using energy-filtered ICP magnetic sector multiple collector mass spectrometry. *Intl. J. Mass Spectrom. Ion Processes* **171,** 105–117.

Marty B., Trull T., Lussiez P., Basile I., and Tanguy J. C. (1994) He, Ar, O, Sr and Nd isotope constraints on the origin and evolution of Mount Etna magmatism. *Earth Planet Sci. Lett.* **126,** 23–39.

McKenzie D. (1985) The extraction of magma from the crust and mantle. *Earth Planet. Sci. Lett.* **74,** 81–91.

McKenzie D. and Bickle M. J. (1988) The volume and composition of melt generated by extension of the lithosphere. *J. Petrol.* **29,** 625–679.

Melson W. G., Thompson G., and van Andel T. H. (1968) Volcanism and metamorphism in the Mid-Atlantic Ridge, 22°N latitude. *J. Geophys. Res.* **73** (*18*)**,** 5925–5941.

Paslick C. R., Halliday A. N., Lange R. A., James D., and Dawson J. B. (1996) Indirect crustal contamination: Evidence from isotopic and chemical disequilibria in minerals from alkali basalts and nephelinites from northern Tanzania. *Contrib. Mineral. Petrol.* **125,** 277–292.

Polve M. and Allegre C. J. (1980) Orogenic lherzolite complexes studied by ^{87}Rb-^{87}Sr: A clue to understand the mantle convection processes? *Earth Planet. Sci. Lett.* **51,** 71–93.

Reisberg L. and Zindler A. (1986) Extreme isotopic variability in the upper mantle: Evidence from Ronda. *Earth Planet. Sci. Lett.* **81,** 29–45.

Resmini R. G. and Marsh B. D. (1995) Steady-state volcanism, paleoeffusion rates, and magma system volume inferred from plagioclase crystal size distributions in mafic lavas: Dome Mountain, Nevada. *J. Volcanol. Geotherm. Res.* **68,** 273–296.

Ribe N. M. (1985) The generation and composition of partial melts in the earth's mantle. *Earth Planet. Sci. Lett.* **73,** 361–376.

Richter F. M. and McKenzie D. (1984) Dynamical models for melt segregation from a deformable matrix. *J. Geol.* **92,** 729–740.

Romano R. (1982) Succession of the volcanic activity in the Etnean area. *Mem. Soc. Geol. Ital.* **23,** 27–48.

Rose E. F., Shimizu N., Layne G. D., and Grove T. L. (2001) Melt production beneath Mt. Shasta from boron data in primitive melt inclusions. *Science* **293,** 281–284.

Russell W. A., Papanastassiou D. A., and Tombrello T. A. (1978) Ca isotope fractionation on the earth and other solar system materials. *Geochim. Cosmochim. Acta* **42,** 1075–1090.

Saal A. E., Hart S. R., Shimizu N., Hauri E. H., and Layne G. D. (1998) Pb Isotopic Variability in Melt inclusions from Oceanic Island Basalts, Polynesia. *Science* **282,** 1481–1484.

Shaw H. R. (1980) The fracture mechanisms of magma transport from the mantle to the surface. In *Physics of Magmatic Processes* (ed. R. B. Hargraves). pp. 201–264, Princeton University Press.

Simonetti A. and Bell K. (1994) Isotopic disequilibrium in clinopyroxenes from nephelinitic lavas. Napak volcano, eastern Uganda. *Geology* **21,** 243–246.

Sobolev A. V., Hofmann A. W., and Nikogosian I. K. (2000) Recycled oceanic crust observed in 'ghost plagioclase' within the source of Mauna Loa lavas. *Nature* **404,** 986–990.

Sours-Page R., Johnson K. T. M., Nielsen R. L., and Karsten J .L. (1999) Local and regional variation of MORB parent magmas: Evidence from melt inclusions from the Endeavour Segment of the Juan de Fuca Ridge. *Contrib. Mineral. Petrol.* **134,** 352–363.

Spiegelman M. (1996) Geochemical consequences of melt transport in 2-D: The sensitivity of trace elements to mantle dynamics. *Earth Planet. Sci. Lett.* **139,** 115–132.

Spiegelman M. and Kelemen P. B. (2003) Extreme chemical variability as a consequence of channelized melt transport. *Geochem. Geophys. Geosyst.* **4,** 1055.

Stewart B. W. and DePaolo D. J. (1990) Isotopic studies of processes in mafic magma chambers: II. The Skaergaard intrusion, East Greenland. *Contrib. Mineral. Petrol.* **104,** 125–141.

Stewart B. W. and DePaolo D. J. (1996) Isotopic studies of processes in mafic magma chambers: III, the Muskox Intrusion, Northwest Territories, Canada. In *Earth Processes: Reading the Isotopic Code,* pp. 277–292. (eds. A. Basu and S. Hart), Geophysical Monograph 95.

Tanguy J. C., Condomines M., and Kieffer G. (1997) Evolution of the Mount Etna magma: Constraints on the present feeding system and eruptive mechanism. *J. Volcanol. Geotherm. Res.* **75,** 221–250.

Tepley F. J., Davidson J. P., and Clynne M. A. (1999) Magmatic interactions as recorded in plagioclase phenocrysts of Chaos Crags, Lassen Volcanic Center, California. *J. Petrol.* **40,** 787–806.

Thirlwall M. F. (2000) Inter-laboratory and other errors in Pb isotope analyses investigated using a ^{207}Pb-^{204}Pb double spike. *Chem. Geol.* **163,** 299–322.

Todt W., Cliff R. A., Hanser A. and Hofmann A. W. (1996) Evaluation of a ^{202}Pb-^{205}Pb double spike for high-precision lead isotope analysis. In *Earth Processes: Reading the Isotopic Code,* pp. 429–437. (eds. A. Basu and S. Hart), Geophysical Monograph 95.

Trua T., Laurenzi M. A., and Oddone M. (1997) Geochronology of the Plio-Pleistocene Hyblean volcanism (SE Sicily): New ^{40}Ar/^{39}Ar data. *Acta Vulcanol.* **9,** 167–176.

Trua T., Esperança S., and Mazzuoli R. (1998) The evolution of the lithospheric mantle along the N African Plate: Geochemical and isotopic evidence from the tholeiitic and alkaline volcanic rocks of the Hyblean plateau, Italy. *Contrib. Mineral. Petrol.* **131,** 307–322.

Turcotte D. L. and Schubert G. (1982) Geodynamics: Applications of Continuum Physics to Geological Problems. Wiley.

Van Orman J. A., Grove T., and Shimizu N. (2002) Diffusive fractionation of trace elements during production and transport of melt in Earth's upper mantle. *Earth Planet Sci. Lett.* **198,** 93–112.

Wagner T. P. and Grove T. L. (1998) Melt/harzburgite reaction in the petrogenesis of tholeiitic magma from Kilauea volcano, Hawaii. *Contrib. Mineral. Petrol.* **131,** 1–12.

West M., Menke W., Tolstoy M., Webb S., and Sohn R. (2001) Magma storage beneath Axial volcano on the Juan de Fuca mid-ocean ridge. *Nature* **413,** 833–836.

Xu Y., Mercier J. -C. C., Menzies M. A., Ross J. V., Harte B., Lin C., and Shi L. (1996) K-rich glass-bearing wehrlite xenoliths from Yitong, Northeastern China: Petrological and chemical evidence for mantle metasomatism. *Contrib. Mineral. Petrol.* **125,** 406–420.

Zindler A., Staudigel H., and Batiza R. (1984) Isotope and trace element geochemistry of young Pacific seamounts: Implications for the scale of upper mantle heterogeneity. *Earth Planet. Sci. Lett.* **70,** 175–195.

Zindler A. and Hart S. (1986) Chemical geodynamics. *Ann Rev. Earth Planet Sci.* **14,** 493–571.